

# On the Curse of Memory in Recurrent Neural Networks: Approximation and Optimization Analysis

Zhong Li <sup>†1</sup>, Jiequn Han <sup>†2</sup>, Weinan E<sup>2</sup>, and Qianxiao Li <sup>‡3,4</sup>

<sup>1</sup>School of Mathematical Science, Peking University

<sup>2</sup>Department of Mathematics and PACM, Princeton University

<sup>3</sup>Department of Mathematics, National University of Singapore

<sup>4</sup>Institute of High Performance Computing, A\*STAR, Singapore

September 17, 2020

## Abstract

We study the approximation properties and optimization dynamics of recurrent neural networks (RNNs) when applied to learn input-output relationships in temporal data. We consider the simple but representative setting of using continuous-time linear RNNs to learn from data generated by linear relationships. Mathematically, the latter can be understood as a sequence of linear functionals. We prove a universal approximation theorem of such linear functionals, and characterize the approximation rate and its relation with memory. Moreover, we perform a fine-grained dynamical analysis of training linear RNNs, which further reveal the intricate interactions between memory and learning. A unifying theme uncovered is the non-trivial effect of memory, a notion that can be made precise in our framework, on approximation and optimization: when there is long term memory in the target, it takes a large number of neurons to approximate it. Moreover, the training process will suffer from slow downs. In particular, both of these effects become exponentially more pronounced with memory - a phenomenon we call the “curse of memory”. These analyses represent a basic step towards a concrete mathematical understanding of new phenomenon that may arise in learning temporal relationships using recurrent architectures.

## 1 Introduction

Recurrent neural networks (RNN) [RHW86] are among the most frequently employed tools to build machine learning models on temporal data. Despite its ubiquitous application in many domains [BBF<sup>+</sup>99, GS09, Gra13, GMH13, GJ14, GDG<sup>+</sup>15], some fundamental theoretical questions remain to be answered. Such questions come in several flavors. First, one may pose the *approximation* problem, which essentially ask what kind of input-output relationships can RNNs model to arbitrary precision. Second, one may also consider the *optimization* problem, which concerns the dynamics of training (say, by gradient descent) the RNN. While such questions can be posed for any machine learning model, the crux of the problem for RNNs is how the recurrent structure of the model and the dynamical nature of the data shape the answers to such problems. For example, it is often claimed that when there are long term dependencies in the data [BSF94, HBFS01], then RNN may encounter problems in learning, but such statements have rarely been put on precise mathematical footing.

In this paper, we make a step in this direction by studying the approximation and optimization properties of RNNs. Compared with their feed-forward counterparts, the key distinguishing feature of RNNs is the presence of temporal dynamics in terms of recurrent architectures and the structure of the data. Hence, to understand the influence of dynamics on learning is of fundamental importance. As is often the case, the key effects of dynamics can already be revealed in the simplest setting of linear dynamics. For this reason, we will focus our analysis on linear RNNs, i.e.

---

<sup>†</sup>Equal contribution

<sup>‡</sup>Corresponding author: qianxiao@nus.edu.sg

those with linear activations. In this case, the RNNs serve to approximate relationships represented by sequences of linear functionals. On first look the setting appears to be simple, but we show that it is very interesting and yields representative results that underlies key differences in the dynamical setting as opposed to static supervised learning problems. In fact, we show that memory, which can be made precise by the decay rates of the target linear functionals, can affect both approximation rates and optimization dynamics in a non-trivial way.

We will employ a continuous-time analysis initially studied in the context of feed-forward architectures [E17, HR17, LCTE17, LH18] and recently in recurrent settings [CAL19, CCHC19, Lim20, She18, NHC19, HKT20, RCD19] and idealize the RNN as a continuous-time dynamical system that depends on the trainable parameters. This allows us to phrase the problems under investigation in convenient analytical settings that accentuates the effect of dynamics.

Our main results are: 1) we give a systematic analysis of the approximation of linear functionals by continuous-time linear RNNs, including a precise characterization of the approximation rates in terms of regularity and memory of the target functional; and 2) We give a fine-grained analysis of the optimization dynamics when training linear RNNs, and show that the training efficiency is adversely affected by the presence of long term memory. These results together paint a comprehensive picture of the interaction of learning and dynamics, and makes concrete the heuristic observations that the presence of long term memory affects RNN learning in a negative manner [BSF94, HBFS01]. In particular, we introduce the concept of the *curse of memory* that mirrors the classical concept of the curse of dimensionality [Bel57]. The former is found to be present in both approximation and optimization aspects of the problem: when there is long term memory in the data, one requires an exponentially large number of neurons for approximation, and the learning dynamics suffers from exponential slow downs. These results form a basic step towards a mathematical understanding of the recurrent structure and its effects on learning from temporal data.

The rest of the paper is organized as follows. We first introduce our problem setting in Section 2. Then, we outline the approximation problem and present our main approximation results in Section 3. The remaining analyses then focuses on the optimization problem in Section 4.

**Notation.** For consistency we will adhere where possible to the following notation. Bold-face letters are reserved for paths, i.e. functions of time, where as lower case letters can mean vectors or scalars. Matrices are denoted by capital letters. Superscript with a parenthesis denotes derivatives, i.e.  $y^{(k)}(t)$  means  $d^k/dt^k y(t)$ .

## 2 Problem Formulation

The basic problem of supervised learning on time series data is to learn a mapping from an input sequence to an output, which may be a single scalar/vector or also a temporal sequence of such values. Formally, one can think of the output as being produced from the input via an unknown function that depends on the entire input sequence, at least up to the time at which the prediction is made. In the discrete-time case, one can write

$$y_k = H_k(x_0, \dots, x_k), \tag{1}$$

where  $\{H_k : k = 0, 1, \dots\}$  is a sequence of functions of increasing input dimension accounting for temporal evolution. The goal of supervised learning is to learn an approximation of  $H_K$  (single target case at step  $K$ ) or  $\{H_k : k = 0, \dots, K\}$  (sequence to sequence case) given observation data.

Recurrent neural networks (RNN) [RHW86] gives a natural way to parameterize such a sequence of functions. In the simplest case, the one-layer RNN is given by

$$\begin{aligned} h_{k+1} &= \sigma(W h_k + U x_k), \\ \hat{y}_{k+1} &= c^\top h_k. \end{aligned} \tag{2}$$

Here,  $\{h_k\}$  are the *hidden states* and its evolution is governed by a feed-forward neural work. Note that we do not include a bias term in the neural network as it can be absorbed into the hidden states. Also, the last output layer can also be non-linear, but we will consider the simplest linear setting. For each time step  $k$ , the mapping  $\{x_0, \dots, x_k\} \mapsto \hat{y}_k$  parameterizes a function  $\hat{H}_k(\cdot)$  through adjustable parameters  $(c, W, U)$ . Hence, for a particular choice of these parameters, a sequence of functions  $\{\hat{H}_k\}$  is constructed at the same time.

The primary question one can ask is, can  $\{\hat{H}_k\}$ , through adjusting  $(c, W, U)$ , approximate any arbitrary sequence of target functions  $\{H_k\}$  using the same set of parameters? If so, what structure in the latter makes the approximation process easy or difficult? Another question one can ask is, what is the dynamics of learning  $(c, W, U)$  by gradient descent, and what properties of the system affects such dynamics? It is the purpose of this paper to investigate such questions in a precise and systematic manner.

The RNN (2) is not easy to analyze due to its discrete iterative nature. Hence, here we employ a continuous-time idealization that replaces the time-step index  $k$  by a continuous time parameter  $t$ . The key advantage of this approach is that the previously motivated questions can be investigated under a unified framework, borrowing useful tools from approximation theory, functional analysis and asymptotic analysis. Let us now introduce this framework.

## 2.1 Continuous-time Formulation

Now, let us consider a sequence of inputs indexed by a real-valued variable  $t \in \mathbb{R}$  instead of a discrete variable  $k$  considered previously. We will assume that the input signal is continuous in  $t$ , giving a natural input space

$$\mathcal{X} = C_0(\mathbb{R}, \mathbb{R}^d), \quad (3)$$

which is the linear space of continuous functions from  $\mathbb{R}$  (time) to  $\mathbb{R}^d$  that vanishes at infinity. We will equip  $\mathcal{X}$  with the supremum norm

$$\|\mathbf{x}\|_{\mathcal{X}} := \sup_{t \in \mathbb{R}} \|x_t\|_{\infty}. \quad (4)$$

For the space of outputs we will take a scalar time series, i.e. the space of bounded continuous functions from  $\mathbb{R}$  to  $\mathbb{R}$ :

$$\mathcal{Y} = C_b(\mathbb{R}, \mathbb{R}). \quad (5)$$

Vector-valued outputs can be handled by considering each output separately, and will not be explicitly treated in the following analyses. To denote paths without ambiguity, we will hereafter adopt the shorthand  $\mathbf{x}_{s:t} := \{x_r : r \in [s, t]\}$ . Similarly, we write  $\mathbf{x}_{:s} := \{x_r : -\infty < r \leq s\}$  and similarly,  $\mathbf{x}_s := \{x_r : s \leq r < \infty\}$ . Finally we write  $\mathbf{x} := \{x_r : r \in \mathbb{R}\} \in \mathcal{X}$ . Similar notation will be used for  $\mathbf{y} \in \mathcal{Y}$ .

To specify the target, we consider a ground truth relationship between inputs  $\mathbf{x}$  and outputs  $\mathbf{y}$  as

$$y_t = H_t(\mathbf{x}), \quad (6)$$

where for each  $t \in \mathbb{R}$ ,  $H_t$  is a functional

$$H_t : \mathcal{X} \rightarrow \mathbb{R}. \quad (7)$$

Let us assume for the moment that the family of functionals  $\{H_t : t \in \mathbb{R}\}$  satisfies the continuity condition

$$\lim_{\delta \rightarrow 0} H_{t+\delta}(\mathbf{x}) = H_t(\mathbf{x}) \quad \text{for all } t \in \mathbb{R}, \mathbf{x} \in \mathcal{X}. \quad (8)$$

This ensures that  $y_t = H_t(\mathbf{x})$  is continuous in  $t$  and so that  $\mathbf{y} \in \mathcal{Y}$  as long as boundedness is satisfied. Later we will show that this is a consequence of other restrictions we may wish to place on the family.

Following the continuous-time viewpoint, we can then define a continuous version of (2) as a hypothesis space to model continuous-time functionals.

$$\begin{aligned}\hat{y}_t &= c^\top h_t, \\ \frac{d}{dt}h_t &= \sigma(Wh_t + Ux_t),\end{aligned}\tag{9}$$

where each  $h_t \in \mathbb{R}^m$  denotes a hidden (latent) state with dimension  $m$  and  $\sigma$  is a point-wise activation function. The dynamics then naturally defines a hypothesis space of sequences of functionals

$$\{\hat{H}_t(\mathbf{x}) = \hat{y}_t : t \in \mathbb{R}\}\tag{10}$$

which can be used to approximate the target functionals  $\{H_t\}$  via adjusting  $(c, W, U)$ .

**Remark 2.1.** *It is worth noting that when viewed in this setting, the RNN parameterization of a family of functionals is in some sense a reverse of the Mori-Zwanzig formalism in statistical mechanics [Zwa01]. In the latter, one passes from a fully observed dynamical system, via introducing memory, to model a closed dynamics involving a subset of relevant observables. For the RNN, the reverse process occurs where one models a input-output relationship with memory by introducing a hidden, but autonomous forced dynamical system. This connection has been pointed out in [MWE18]. Thus, a thorough understanding of the behavior of RNNs may also contribute towards developing practical implementations of the Mori-Zwanzig formalism for physical applications.*

Clearly, the family of functionals the RNN can represent is not arbitrary, and must possess some structure. Let us now introduce some definitions of functionals that makes these structures precise.

The first is the idea of causality, which means that each functional  $H_t$  should only depend on the input time sequence up to time  $t$ .

**Definition 2.1** (Causal Functionals). *We call  $H_t$  a causal functional if it does not depend on the future values of  $\mathbf{x}$ . Concretely,  $H_t$  is causal if for every pair of  $\mathbf{x}, \mathbf{x}' \in \mathcal{X}$  such that*

$$x_s = x'_s \text{ for all } s \leq t,\tag{11}$$

*we must have  $H_t(\mathbf{x}) = H_t(\mathbf{x}')$ .*

Next, the primary object of study in this paper are (continuous) linear functionals, which we define below.

**Definition 2.2** (Continuous Linear Functionals). *We call  $H$  a continuous linear functional if for any  $\mathbf{x}, \mathbf{x}' \in \mathcal{X}$  and  $\lambda, \lambda' \in \mathbb{R}$  we have*

$$H(\lambda\mathbf{x} + \lambda'\mathbf{x}') = \lambda H(\mathbf{x}) + \lambda' H(\mathbf{x}')\tag{12}$$

*and moreover that*

$$\sup_{\mathbf{x} \in \mathcal{X}, \|\mathbf{x}\|_{\mathcal{X}} \leq 1} H(\mathbf{x}) < \infty,\tag{13}$$

*in which case we can define the induced norm as*

$$\|H\| := \sup_{\mathbf{x} \in \mathcal{X}, \|\mathbf{x}\|_{\mathcal{X}} \leq 1} |H(\mathbf{x})|, \quad H \in \mathcal{X}^*.\tag{14}$$

*We say that a family  $\{H_t\}$  is continuous and linear if each  $H_t$  is continuous and linear.*

We end with two other properties that functionals that can satisfy, that are especially of relevance to RNNs.

**Definition 2.3** (Regular Functionals). *We say that a functional  $H : \mathcal{X} \rightarrow \mathbb{R}$  is regular if for any sequence  $\{\mathbf{x}^{(n)} \in \mathcal{X}, : n \geq 0\}$  such that  $x_t^{(n)} \rightarrow 0$  for almost every  $t \in \mathbb{R}$  (in the sense of Lebesgue measure), then*

$$\lim_{n \rightarrow \infty} H(\mathbf{x}_n) = 0.\tag{15}$$

*We say that the family  $\{H_t\}$  is regular if each  $H_t$  is regular.*

**Definition 2.4** (Time-homogeneous Functionals). We say a family of functionals  $\{H_t : t \in \mathbb{R}\}$  is time-homogeneous if for every  $t, \tau \in \mathbb{R}$ , we have

$$H_t(\mathbf{x}) = H_{t+\tau}(\mathbf{x}^{(\tau)}) \quad (16)$$

where  $x_s^{(\tau)} = x_{s-\tau}$  for all  $s$ , i.e.  $\mathbf{x}^{(\tau)}$  is  $\mathbf{x}$  whose time index is shifted to the right by  $\tau$ .

One can think of regular functionals as those that are not determined by values of the inputs on an arbitrarily small time interval, e.g. a thin spike. Time-homogeneous functionals, on the other hand, are those where there is no special reference point in time: if the time index of both the input sequence and the functional are shifted in a coordinated way, then the output value remains the same.

### 3 Approximation Theory for Linear RNNs

In this section we develop an approximation theory of functionals by RNNs. We first introduce the basic approximation setting. In continuous time, the linear RNN obeys the following dynamics

$$\begin{aligned} \hat{y}_t &= c^\top h_t, \\ \frac{dh_t}{dt} &= Wh_t + Ux_t. \end{aligned} \quad (17)$$

Notice that in the theoretical setup, the initial time of the system goes back to  $-\infty$  with  $\lim_{t \rightarrow -\infty} x_t = 0, \forall \mathbf{x} \in \mathcal{X}$ , thus by linearity ( $H_t(\mathbf{0}) = 0$ ) we specify the initial condition of the hidden state  $h_{-\infty} = 0$  for consistency. In this case, the equation eq. (17) has the following solution

$$\hat{y}_t = \int_0^\infty c^\top e^{Ws} Ux_{t-s} ds. \quad (18)$$

We will mainly consider stable RNNs, where  $W \in \mathcal{W}_m$  with

$$\mathcal{W}_m = \{W \in \mathbb{R}^{m \times m} : \text{eigenvalues of } W \text{ have negative real parts}\}. \quad (19)$$

Owing to the representation of solutions in eq. (18), the linear RNN defines a family of functionals

$$\begin{aligned} \hat{\mathcal{H}} &:= \cup_{m \geq 1} \hat{\mathcal{H}}_m \\ \hat{\mathcal{H}}_m &:= \left\{ \{\hat{H}_t(\mathbf{x}), t \in \mathbb{R}\} : \hat{H}_t(\mathbf{x}) = \int_0^\infty c^\top e^{Ws} Ux_{t-s} ds, W \in \mathcal{W}_m, U \in \mathbb{R}^{m \times d}, c \in \mathbb{R}^m \right\} \end{aligned} \quad (20)$$

The most basic approximation problem is as follows: given some sequence of target functionals  $\{H_t : t \in \mathbb{R}\}$  satisfying appropriate conditions, does there always exist a sequence of RNN functionals  $\{\hat{H}_t : t \in \mathbb{R}\}$  in  $\hat{\mathcal{H}}$  such that  $H_t \approx \hat{H}_t$  for all  $t \in \mathbb{R}$ ?

We now make an important remark with respect to the current problem formulation that differs from previous investigations in RNN approximation: we are **not** assuming that the target functionals  $\{H_t : t \in \mathbb{R}\}$  are themselves generated from an underlying dynamical system. In other words, there may be no dynamical systems satisfying

$$H_t(\mathbf{x}) = y_t \quad \text{where} \quad \begin{aligned} y_t &= g(h_t) \\ \frac{d}{dt} h_t &= f(h_t, x_t) \end{aligned} \quad (21)$$

for any linear or nonlinear functions  $f, g$ . This sets apart our current setting with previous work on approximation theory of RNNs [Mat93, NN09, CX00, LHC05, SZ06, SZ07, iFN93] (and also RNN training dynamics [HMR18]), where it is assumed that the sequence of target functionals are indeed generated from some unknown dynamical system.

In this setting, the approximation problem reduces to the approximation of the functions  $f, g$  of the underlying dynamical system by neural networks, and the obtained results often resemble those in feed-forward networks.

In our case, however, we consider general input-output relationships related by temporal sequences of functionals, with no necessary recourse to the mechanism from which these relationships are generated. This is an important distinction, for often in RNN applications, the time-series data may not be generated from some partially observed Markovian process. Hence, this setting is more general, and natural for applications. Moreover, notice that in the linear case, if the target functionals  $\{H_t\}$  are generated from a linear dynamical system, then the approximation question is trivial: as long as  $h_t$ 's dimension in the approximating RNN is greater than or equal to that which generates the target, we have perfect approximation. However, we will see that in the more general consideration of approximation a sequence of target functionals, this question becomes much more interesting, even in the linear regime. In fact, we will now prove precise approximation theories and characterize approximation rates that reveal intricate connections with memory effects, which may be otherwise obscured if one considers more limited settings of recovering hidden dynamical systems.

### 3.1 Universal Approximation Theorem of Linear Functionals by Linear RNNs

First, it is clear that the functionals in RNN hypothesis  $\hat{\mathcal{H}}$  space must possess some structure, which motivated the introduction of various classes of functionals in section 2.1. The following observation can be verified directly and its proof is immediate and hence omitted.

**Proposition 3.1.** *Let  $\{\hat{H}_t : t \in \mathbb{R}\}$  be any family of functionals in  $\hat{\mathcal{H}}$  (eq. (20)) resulting from the linear RNN dynamics (9). Then for each  $t \in \mathbb{R}$ ,*

1.  $\hat{H}_t$  is a continuous, linear functional.
2.  $\hat{H}_t$  is a causal functional.
3.  $\hat{H}_t$  is a regular functional.
4. The family  $\{\hat{H}_t\}$  is time-homogeneous.

Our first main result is in some sense a converse of Prop. 3.1. In particular, we prove the following approximation theorem, which says that *any* sequence of functionals satisfying the properties in proposition 3.1 can be approximated uniformly by sequences of RNN functionals in  $\hat{\mathcal{H}}$  to arbitrary accuracy.

**Theorem 3.1** (UAP for Linear RNNs). *Let  $\{H_t : t \in \mathbb{R}\}$  be a family of continuous, linear, causal, regular and time homogeneous functionals on  $\mathcal{X}$ . Then, for any  $\epsilon > 0$  there exists  $\{\hat{H}_t : t \in \mathbb{R}\} \in \hat{\mathcal{H}}$  such that*

$$\sup_{t \in \mathbb{R}} \|H_t - \hat{H}_t\| \equiv \sup_{t \in \mathbb{R}} \sup_{\|\mathbf{x}\|_{\mathcal{X}} \leq 1} |H_t(\mathbf{x}) - \hat{H}_t(\mathbf{x})| \leq \epsilon. \quad (22)$$

We now present the proof of this result. A key simplification of considering linear functionals is due to the classical representation result below, which allows us to pass from the approximation of functionals to the approximation of functions.

**Theorem 3.2** (Riesz-Markov-Kakutani Representation Theorem). *Let  $H : \mathcal{X} \rightarrow \mathbb{R}$  be a continuous linear functional. Then, there exists a unique, vector-valued, regular, countably additive signed measure  $\mu$  on  $\mathbb{R}$  such that*

$$H(\mathbf{x}) = \int_{\mathbb{R}} \mathbf{x}_s^\top d\mu(s) = \sum_{i=1}^d \int_{\mathbb{R}} x_{s,i} d\mu_i(s). \quad (23)$$

Moreover, we have

$$\|H\| := \sup_{\|\mathbf{x}\|_{\mathcal{X}} \leq 1} |H(\mathbf{x})| = \|\mu\|_1(\mathbb{R}) := \sum_i |\mu_i|(\mathbb{R}). \quad (24)$$

*Proof.* Well-known, see e.g. [Bog07], CH 7.10.4. □

We will use the representation theorem to prove the main result. First, We prove some lemmas.

**Lemma 3.1.** *Let  $\{H_t\}$  be a family of continuous, linear, regular, causal and time homogeneous functionals on  $\mathcal{X}$ . Then, there exists a measurable function  $\rho : [0, \infty) \rightarrow \mathbb{R}^d$  that is integrable, i.e.*

$$\|\rho\|_{L^1([0, \infty))} := \sum_{i=1}^d \int_0^\infty |\rho_i(s)| ds < \infty \quad (25)$$

and

$$H_t(\mathbf{x}) = \int_0^\infty x_{t-s}^\top \rho(s) ds, \quad t \in \mathbb{R}. \quad (26)$$

In particular,  $\{H_t\}$  is uniformly bounded with  $\sup_t \|H_t\| = \|\rho\|_{L^1([0, \infty))}$  and  $t \mapsto H_t(\mathbf{x})$  is continuous for all  $\mathbf{x} \in \mathcal{X}$ .

*Proof.* By the Riesz-Markov-Kakutani representation theorem (theorem 3.2), for each  $t$  there is a unique regular signed Borel measure  $\mu_t$  such that

$$H_t(\mathbf{x}) = \int_{\mathbb{R}} x_s^\top d\mu_t(s), \quad (27)$$

and  $\sum_i |\mu_{t,i}|(\mathbb{R}) = \|H_t\|$ . Since  $\{H_t\}$  is causal, we must have  $\int_t^\infty x_s^\top d\mu_t(s) = 0$  for any  $\mathbf{x}$  and thus

$$H_t(\mathbf{x}) = \int_{-\infty}^t x_s^\top d\mu_t(s). \quad (28)$$

Now, by time homogeneity we have

$$\int_{-\infty}^t x_s^\top d\mu_t(s) = H_t(\mathbf{x}) = H_{t+\tau}(\mathbf{x}^{(\tau)}) = \int_{-\infty}^{t+\tau} x_{s-\tau}^\top d\mu_{t+\tau}(s). \quad (29)$$

Take  $\tau = -t$  and set  $\mu = -\mu_0$  to get

$$H_t(\mathbf{x}) = \int_0^\infty x_{t-s}^\top d\mu(s). \quad (30)$$

Note that we have  $\|\mu\|_1([0, \infty)) = \|\mu_0\|_1([0, \infty)) = \|H_0\| = \|H_t\|$ , and continuity follows from the fact that

$$\begin{aligned} |H_{t+\delta}(\mathbf{x}) - H_t(\mathbf{x})| &= \left| \int_0^\infty (x_{t+\delta-s} - x_{t-s})^\top d\mu(s) \right| \\ &\leq \sum_i \int_0^\infty \|x_{t+\delta-s} - x_{t-s}\|_\infty d|\mu_i|(s), \end{aligned} \quad (31)$$

which converges to 0 as  $\delta \rightarrow 0$  by dominated convergence theorem. Finally, we will show that each  $\mu_i$  is absolutely continuous with respect to  $\lambda$  (Lebesgue measure). Take a measurable  $E \subset [0, \infty)$  such that  $\lambda(E) = 0$  and set  $E' = [0, \infty) \setminus E$ . For each  $n \geq 0$  set  $K_n \subset E, K'_n \subset E'$  where  $K_n, K'_n$  are closed and  $\mu_i(E \setminus K_n) \leq 1/n, \mu_i(E' \setminus K'_n) \leq 1/n$ . For a fixed  $i \in \{1, \dots, d\}$ , define  $\mathbf{x}^{(n)}$  to be such that  $x_{t-s,j}^{(n)} = 0$  for all  $j \neq i$  and all  $s$ . For  $j = i$ , we set  $x_{t-s,i}^{(n)} = 1$  if  $s \in K_n$  and 0 if  $s \in K'_n$ , which can then be continuously extended to  $[0, \infty)$ . Observe that by construction,  $x_{t-s}^{(n)} \rightarrow 0$  for  $\lambda$ -a.e.  $s$ , thus by dominated convergence theorem

$$0 = \lim_{n \rightarrow \infty} H_t(\mathbf{x}^{(n)}) = \mu_i(E). \quad (32)$$

This shows that  $\mu_i$  is absolutely continuous with respect to  $\lambda$ , and by the Radon-Nikodym theorem there exists a measurable function  $\rho_i : [0, \infty) \rightarrow \mathbb{R}$  such that for any measurable  $A \subset \mathbb{R}$  we have

$$\int_A d\mu_i(s) = \int_A \rho_i(s) ds, \quad (33)$$

for  $i = 1, \dots, d$ . Hence, we have

$$H_t(\mathbf{x}) = \int_0^\infty x_{t-s}^\top \rho(s) ds \quad (34)$$

with  $\|\rho\|_{L^1([0,\infty))} = \sum_i \int_0^\infty |\rho_i(s)| ds = \|\mu\|_1([0,\infty)) < \infty$ .

□

**Lemma 3.2.** *Let  $\rho : [0, \infty) \rightarrow \mathbb{R}$  a Lebesgue integrable function, i.e.  $\|\rho\|_{L^1([0,\infty))} < \infty$ . Then, for any  $\epsilon > 0$ , there exists a polynomial  $p$  with  $p(0) = 0$  such that*

$$\|\rho - p(e^{-\cdot})\|_{L^1([0,\infty))} = \int_0^\infty |\rho(t) - p(e^{-t})| dt \leq \epsilon. \quad (35)$$

*Proof.* The approach here is similar to that of the approximation of functions using exponential sums [Kam76, Bra86] Fix  $\epsilon > 0$ . Define

$$R(u) = \begin{cases} \frac{1}{u} \rho(-\log u), & u \in (0, 1], \\ 0, & u = 0. \end{cases} \quad (36)$$

Then, we can check that

$$\|R\|_{L^1([0,1])} = \|\rho\|_{L^1([0,\infty))} < \infty. \quad (37)$$

By density of continuous functions in  $L^1$  there exists a continuous function  $\tilde{R}$  on  $[0, 1]$  with  $\tilde{R}(0) = 0$  such that

$$\|R - \tilde{R}\|_{L^1([0,1])} \leq \epsilon/2. \quad (38)$$

By Müntz-Szász theorem [Mün14, Szá16], there exists a polynomial  $p$  with  $p(0) = 0$  such that

$$\|q - \tilde{R}\|_{L^1([0,1])} \leq \epsilon/2, \quad (39)$$

and  $q(u) := p(u)/u$  is also a polynomial. Therefore, we have

$$\begin{aligned} \|\rho - p(e^{-\cdot})\|_{L^1([0,\infty))} &= \int_0^1 |R(u) - p(u)/u| du \\ &\leq \int_0^1 |R(u) - \tilde{R}(u)| du + \int_0^1 |\tilde{R}(u) - p(u)/u| du \leq \epsilon. \end{aligned} \quad (40)$$

□

We are now ready to present the proof of the first main result.

*Proof of theorem 3.1.* By eq. (18), for each  $\{\hat{H}_t\} \in \hat{\mathcal{H}}$  we can write

$$\hat{H}_t(\mathbf{x}) = \int_0^\infty x_{t-s}^\top (U^\top [e^{Ws}]^\top c) ds. \quad (41)$$

By lemma 3.1, we can write

$$H_t(\mathbf{x}) = \int_0^\infty x_{t-s}^\top \rho(s) ds, \quad (42)$$

where  $\rho$  is integrable. Thus, we can apply lemma 3.2 to conclude that there exists polynomials  $p_i, i = 1, \dots, d$  with  $p_i(0) = 0$  such that

$$\sum_i \|\rho_i - p_i(e^{-\cdot})\|_{L^1([0,\infty))} \leq \epsilon. \quad (43)$$



Notice that we can write each  $p_i(u) = \sum_{j=1}^m \alpha_{ij} u^j$  for some  $m$  equaling the maximal order of  $\{p_i\}$ . Taking  $W = \text{diag}(-1, \dots, -m)$ ,  $c = (1, \dots, 1)$  and  $U_{ij} = \alpha_{ji}$ , we have

$$(U^\top [e^{Ws}]^\top c)_i = p_i(e^{-s}), \quad i = 1, \dots, d. \quad (44)$$

Consequently, we have for any  $\mathbf{x}$  with  $\|\mathbf{x}\|_\infty \leq 1$ ,

$$\begin{aligned} |H_t(\mathbf{x}) - \hat{H}_t(\mathbf{x})| &= \left| \int_0^\infty x_{t-s}^\top \rho(s) ds - \int_0^\infty x_{t-s}^\top p(e^{-s}) ds \right| \\ &\leq \sum_i \int_0^\infty |x_{t-s,i}| |\rho_i(s) - p_i(e^{-s})| ds \leq \sum_i \|\rho_i - p_i(e^{-\cdot})\|_{L^1([0, \infty))} \\ &\leq \epsilon. \end{aligned} \quad (45)$$

□

**Remark 3.1.** *Theorem 3.1 can be extended in several ways. Without the assumption of causality, we can use bidirectional recurrent neural networks [SP97] to achieve the universal approximation. Without the assumption of time-homogeneity, we can introduce another coordinate to act as time. Without regularity assumption on  $\{H_t\}$ , we would not have uniform error estimate (i.e.  $\sup_t$ ), in which case we can replace it with some  $L^p$  estimate in time.*

**Remark 3.2.** *In the literature, there are in fact many results on the approximation properties of RNNs in discrete [SZ06, SZ07, Mat93] and continuous time [iFN93, NN09, LHC05, CX00]. However, as discussed before, most of these focus on the case where the target relationship is generated from dynamical systems. The formulation here is more general, and reveals new phenomena that may not be discovered from these approaches. This will be especially apparent in the next section when it comes to approximation rates. We also note that the functional/operator approximation using neural networks has been explored in [CC93, TH95, LJK19], but not in the context of recurrent architectures.*

### 3.2 Approximation Rates

While the previous result establishes the universal approximation property of linear RNNs for suitable classes of linear functionals, it does not reveal to us which functionals can be efficiently approximated. In the practical literature, it is often observed that when there is some long-term memory in the inputs and the outputs, the RNN becomes quite ill-behaved [BSF94, HBFS01]. It is the purpose of this section to establish results which make these heuristics statements precise. In particular, we will show that the rate at which linear functionals can be approximated by RNNs depends on the former's smoothness and memory properties. We note that this is a much less explored area in the approximation theory of RNNs.

To characterize smoothness and decay of functionals, we may pass to investigating the properties of their actions on constant input signals. Concretely, let us denote by  $e_i$  ( $i = 1, \dots, d$ ) the standard basis vector in  $\mathbb{R}^d$ , and  $e_i$  denotes a constant signal with  $e_{i,t} = e_i 1_{\{t \geq 0\}}$  for all  $t$ . Then,

1. smoothness is characterized by the smoothness of the maps  $t \mapsto H_t(e_i)$ ,  $i = 1, \dots, d$
2. memory is characterized by the decay rate of the maps  $t \mapsto H_t(e_i)$ ,  $i = 1, \dots, d$

Our second main result shows that these two properties are intimately tied with the approximation rate.

**Theorem 3.3** (Approximation rate of linear RNN). *Assuming the conditions as in theorem 3.1. Consider the output of constant signal*

$$y_i(t) = H_t(e_i), \quad i = 1, \dots, d. \quad (46)$$

*Suppose there exist constants  $\alpha \in \mathbb{Z}^+$ ,  $\beta, \gamma \in \mathbb{R}^+$  such that for  $i = 1, \dots, d$ ,  $y_i(t) \in C^{(\alpha+1)}(\mathbb{R})$  and for  $k =$*

$1, \dots, \alpha + 1,$

$$e^{\beta t} y_i^{(k)}(t) = o(1) \text{ as } t \rightarrow +\infty, \quad (47)$$

$$\sup_{t \geq 0} \frac{|e^{\beta t} y_i^{(k)}(t)|}{\beta^k} \leq \gamma. \quad (48)$$

Then, there exists a universal constant  $C(\alpha)$  that only depends on  $\alpha$  such that for any  $\epsilon > 0$ , there exists a sequence of width- $m$  RNN functionals  $\{\hat{H}_t : t \in \mathbb{R}\} \in \hat{\mathcal{H}}_m$  such that

$$\sup_{t \in \mathbb{R}} \|H_t - \hat{H}_t\| \equiv \sup_{t \in \mathbb{R}} \sup_{\|\mathbf{x}\|_{\mathcal{X}} \leq 1} |H_t(\mathbf{x}) - \hat{H}_t(\mathbf{x})| \leq \frac{C(\alpha)\gamma d}{\beta m^\alpha}. \quad (49)$$

*Proof.* We fix  $i \in \{1, \dots, d\}$  below until the last part of the proof. By lemma 3.1, there exists  $\rho_i(t) \in C^\alpha[0, \infty)$  such that

$$y_i(t) = H_t(\mathbf{e}_i) = \int_0^t \rho_i(r) dr, \quad t \geq 0. \quad (50)$$

By the assumption,

$$\rho_i^{(k)}(t) = o(e^{-\beta t}) \text{ as } t \rightarrow \infty, \quad k = 0, \dots, \alpha. \quad (51)$$

Consider the transform

$$q_i(s) = \begin{cases} 0 & s = 0, \\ \frac{\rho_i\left(\frac{-(\alpha+1)\log s}{\beta}\right)}{s} & s \in (0, 1]. \end{cases} \quad (52)$$

For  $k = 0, \dots, \alpha$ , one can prove by induction that

$$q_i^{(k)}(s) = \sum_{j=0}^k c(j, k) \left(-\frac{\alpha+1}{\beta}\right)^j \frac{\rho_i^{(j)}\left(\frac{-(\alpha+1)\log s}{\beta}\right)}{s^{j+1}}, \quad (53)$$

where  $c(j, k)$  are some integer constants. Together with the assumption, we have

$$\left|q_i^{(k)}(e^{-\frac{\beta}{\alpha+1}t})\right| = \left|\sum_{j=0}^k c(j, k) \left(-\frac{\alpha+1}{\beta}\right)^j \frac{\rho_i^{(j)}(t)}{e^{-\frac{(j+1)\beta}{\alpha+1}t}}\right| \leq \sum_{j=0}^k |c(j, k)| (\alpha+1)^j \gamma \leq C(\alpha)\gamma, \quad (54)$$

where  $C(\alpha)$  is a universal constant only depending on  $\alpha$ . Note that for  $j = 0, \dots, \alpha$ ,

$$\lim_{s \rightarrow 0^+} \frac{\rho_i^{(j)}\left(\frac{-(\alpha+1)\log s}{\beta}\right)}{s^{j+1}} = \lim_{t \rightarrow \infty} \frac{\rho_i^{(j)}(t)}{e^{-\frac{(j+1)\beta}{\alpha+1}t}} = \lim_{t \rightarrow \infty} \frac{\rho_i^{(j)}(t)}{e^{-\beta t}} e^{-\frac{(\alpha-j)\beta}{\alpha+1}t} = 0, \quad (55)$$

hence  $q_i(s) \in C^\alpha[0, 1]$  with  $q_i(0) = q_i^{(1)}(0) = \dots = q_i^{(\alpha)}(0) = 0$ . By Jackson's theorem [Jac30], for  $m = 1, 2, \dots$ , there exists a polynomial  $Q_{i,m}$  of degree  $m - 1$  such that

$$\|q_i - Q_{i,m}\|_{L^\infty([0,1])} \leq \frac{C(\alpha)\gamma}{m^\alpha}. \quad (56)$$

Denote the polynomial  $Q_{i,m}$  as

$$Q_{i,m}(s) = \sum_{j=0}^{m-1} \alpha_{i,j} s^j, \quad (57)$$

and define

$$\phi_{i,m}(t) = e^{-\frac{\beta}{\alpha+1}t} Q_{i,m}(e^{-\frac{\beta}{\alpha+1}t}). \quad (58)$$

Then we have

$$\phi_{i,m}(t) = c^\top e^{Wt} u_i, \quad (59)$$

where

$$c = (1, 1, \dots, 1), \quad (60)$$

$$W = \begin{bmatrix} -\frac{\beta}{\alpha+1} & & & \\ & -\frac{2\beta}{\alpha+1} & & \\ & & \ddots & \\ & & & -\frac{m\beta}{\alpha+1} \end{bmatrix}, \quad (61)$$

$$u_i = (\alpha_{i,0}, \alpha_{i,1}, \dots, \alpha_{i,m-1}). \quad (62)$$

With a change of variable  $s = e^{-\frac{\beta}{\alpha+1}t}$ , we have the estimate

$$\begin{aligned} \|\rho_i - \phi_{i,m}\|_{L^1([0,\infty))} &= \int_0^\infty |\rho_i(t) - \phi_m(t)| dt \\ &= \int_0^1 \left| \rho_i \left( \frac{-(\alpha+1) \log s}{\beta} \right) - s Q_{i,m}(s) \right| \frac{\alpha+1}{\beta s} ds \\ &= \frac{\alpha+1}{\beta} \int_0^1 |q_i(s) - Q_{i,m}(s)| ds \\ &\leq \frac{C(\alpha)\gamma}{\beta m^\alpha}. \end{aligned} \quad (63)$$

Finally we define  $U = [u_1, \dots, u_d] \in \mathbb{R}^{m \times d}$  and have

$$c^\top e^{Wt} U = (\phi_{1,m}(t), \dots, \phi_{d,m}(t)). \quad (64)$$

Parameters  $c, W, U$  together determine the dynamical system eq. (9). Similar to the argument in the proof of theorem 3.1, for any  $\mathbf{x}$  with  $\|\mathbf{x}\|_\infty \leq 1$  and  $t$ , we have

$$|H_t(\mathbf{x}) - \hat{H}_t(\mathbf{x})| \leq \sum_i \|\rho_i - \phi_{i,m}\|_{L^1([0,\infty))} \leq \frac{C(\alpha)\gamma d}{\beta m^\alpha}. \quad (65)$$

□

### 3.3 The curse of memory in approximation

For approximation of non-linear functions using linear combinations of basis functions, one often suffers from the ‘‘curse of dimensionality’’ [Bel57], in that the number of basis functions required to achieve a certain approximation accuracy increases exponentially when the dimension  $d$  of the input space increases. In the case of Theorem 3.3, the bound scales linearly with  $d$  (See eq. (49)). This is because the target functional possesses a linear structure, and hence each dimension can be approximated independently of others, resulting in an additive error estimate. Nevertheless, due to the presence of the temporal dimension, there enters another type of challenge, which we coin the *curse of memory*. Let us now discuss this point in detail.

We assume  $d = 1$  and drop subscripts for simplicity and consider an example in which the density (defined in eq. (50)) satisfies  $\rho(t) \in C^{(1)}(\mathbb{R})$  and

$$\rho(t) \sim t^{-(1+\omega)} \text{ as } t \rightarrow +\infty. \quad (66)$$

Here  $\omega > 0$  indicates the decay rate of the memory effects in our target functional family  $\{H_t\}$ . The smaller its value, the slower the decay and the longer the system memory. Notice that  $y^{(1)}(t) = \rho(t)$  and in this case there exists no  $\beta$  making eq. (47) true, and no rate estimate can be deduced from it.

A natural way to circumvent this obstacle is to introduce a truncation in time. With  $T (\gg 1)$  we can define  $\tilde{\rho}(t) \in C^{(1)}(\mathbb{R})$  such that  $\tilde{\rho}(t) \equiv \rho(t)$  for  $t \leq T$ ,  $\tilde{\rho}(t) \equiv 0$  for  $t \geq T+1$ , and  $\tilde{\rho}(t)$  is monotonly decreasing for  $T \leq t \leq T+1$ . Considering the linear functional

$$\tilde{H}_t(\mathbf{x}) := \int_0^t x_{t-s} \tilde{\rho}(s) ds, \quad (67)$$

we have the truncation error estimate

$$|H_t(\mathbf{x}) - \tilde{H}_t(\mathbf{x})| \leq \|\mathbf{x}\|_{\mathcal{X}} \left( \int_T^\infty |\rho(s)| ds \right) \sim \|\mathbf{x}\|_{\mathcal{X}} T^{-\omega}. \quad (68)$$

Now Theorem 3.3 is applicable to the truncated  $\{\tilde{H}_t\}$  (with  $\alpha = 1$ ), and we have for  $\forall \beta > 0$ , there is a linear RNN  $(U, W, c)$  such that the associated functionals  $\{\hat{H}_t\} \in \hat{\mathcal{H}}_m$  satisfy

$$\sup_{t \in \mathbb{R}} \|\tilde{H}_t - \hat{H}_t\| \leq \frac{C\gamma}{\beta m} := \frac{C}{\beta m} \sup_{t \geq 0} \frac{|e^{\beta t} y^{(1)}(t)|}{\beta} = \frac{C\omega}{m} \frac{e^{\beta T}}{\beta^2 T^{\omega+1}}. \quad (69)$$

It is straightforward to verify that when  $\beta = 2/T$ , the right-hand side of eq. (69) achieves the minimum, which gives us

$$\sup_{t \in \mathbb{R}} \|\tilde{H}_t - \hat{H}_t\| \leq \frac{C\omega}{m} T^{1-\omega}. \quad (70)$$

Combining eqs. (68) and (70) gives us

$$\sup_{t \in \mathbb{R}} \|\tilde{H}_t - \hat{H}_t\| \leq C \left( T^{-\omega} + \frac{\omega}{m} T^{1-\omega} \right). \quad (71)$$

In order to achieve an error tolerance  $\epsilon$ , according to the first term above we require  $T \sim \epsilon^{-\frac{1}{\omega}}$ , and then according to second term we have

$$m = \mathcal{O} \left( \frac{\omega T^{1-\omega}}{\epsilon} \right) = \mathcal{O} \left( \omega \epsilon^{-\frac{1}{\omega}} \right). \quad (72)$$

This estimate gives us a quantitative relationship between the degree of freedom needed and the decay speed. When  $\omega$  is small, i.e., the system has long memory, the size of the RNN required grows exponentially. This is akin to the curse of dimensionality, but this time on memory, which manifests itself even in the simplest linear settings.

**Remark 3.3.** *Here, the curse of memory is on approximation properties, in that functionals with long memory are hard to approximate by the RNN architecture. This is unrelated to the commonly quoted idea of "vanishing and explosion of gradients" [PMB13, HR18, Han18] that plagues RNNs (and indeed many deep architectures). In fact, the curse of memory for approximation is inherent in the architecture itself, without reference to any training algorithm. At the same time, this is also specific to RNNs when viewed as approximators of functionals.*

**Remark 3.4.** *The result here also highlights the importance of considering the approximation of general sequences of functionals, instead of those generated by underlying dynamical systems. In the latter case, approximation theory reduces to the function approximation regime of feed-forward networks, and the approximation rates one obtains may not capture the dynamical aspect of the problem and reveal the curse of memory associated with it.*

## 4 Fine-grained Analysis of Optimization Properties of Linear RNNs

In the previous sections we gave a general characterization of the approximation of linear functionals using linear RNNs. It is revealed that memory plays an important role in determining the approximation rates. The result therein only depends on the architecture, and does not concern the actual training dynamics. In this section, we turn our attention to the optimization problem and perform a fine-grained analysis of the dynamics of the training process when applying linear RNNs to learn linear functionals. In this case, we again find an interesting interaction between memory and learning dynamics. These results then puts the ubiquitous but heuristic observations - that long term memory negatively impacts training efficiency [BSF94, HBFS01] - on concrete theoretical footing, at least in idealized settings. At the same time, we also complement general results on “vanishing and explosion of gradients” [PMB13, HR18, Han18] that are typically restricted to initialization settings with more precise characterizations in the dynamical regime during training.

To introduce the dynamical analysis we first define the loss function for training. We will use the squared difference between the ground truth functional and the one parameterized by the RNN at time  $T > 0$  averaged over input distributions over  $\mathbf{x}$  (empirical, or population), which can be written as

$$\mathbb{E}_{\mathbf{x}} J_m(\mathbf{x}; c, W, U) := \mathbb{E}_{\mathbf{x}} |\hat{H}_T(\mathbf{x}) - H_T(\mathbf{x})|^2 = \mathbb{E}_{\mathbf{x}} \left| \int_0^T [c^\top e^{Wt} U - \rho(t)^\top] x_{T-t} dt \right|^2. \quad (73)$$

where the input time series  $\mathbf{x}$  is assumed to be finitely cut off, i.e. without loss of generality they satisfy  $x_t = 0$  for any  $t \leq 0$  almost surely. Training the RNN amounts to optimizing  $\mathbb{E}_{\mathbf{x}} J_m$  with respect to the parameters  $c, W, U$ . The most commonly applied method is (stochastic) gradient descent (GD), which updates them in the steepest descent direction.

### 4.1 Motivating Numerical Examples

We first show that the dynamics of GD exhibit very interesting behavior depending on the form of the target functionals. We will take  $d = 1$  and consider two cases:

1. Exponential sum:  $\rho(t) = [c^*]^\top e^{W^* t} b^*$ , where  $c^*, b^*$  are standard normal random vectors of  $m^*$  dimensions and  $W = -I - Z^\top Z$  with  $Z \in \mathbb{R}^{m^* \times m^*}$  a Gaussian random matrix with i.i.d. entries having variance  $1/m^*$ .
2. Airy function:  $\rho(t) = \text{Ai}(s_0[t - t_0])$ , where  $\text{Ai}(t)$  is the Airy function of the first kind, given by the improper integral

$$\text{Ai}(t) = \frac{1}{\pi} \lim_{\xi \rightarrow \infty} \int_0^\xi \cos\left(\frac{u^3}{3} + tu\right) du. \quad (74)$$

Note that in the first example, the target functional’s memory decays quickly. However, for the airy function, the effective rate of decay is controlled by the parameter  $t_0$ . For  $t \leq t_0$ , the airy function is oscillatory and hence for large  $t_0$ , a large amount of memory is present in the target. We now show via numerical experiments that the long memory adversely affects the optimization process via gradient descent. In Figure 1, we plot the dynamics of gradient descent on training the linear RNNs (discretized using Euler method, hence equivalent to residual RNNs). We observe that training proceeds efficiently for the exponential sum case, but in the second airy function case, there are interesting “plateauing” behavior of the loss function, where the loss decrement slows down significantly after some time in training. The plateau is sustained for a long time before further decrements is observed. This causes a severe slow down of training, and this effect gets worse as  $t_0$  (or  $s_0$ ) is increased, which corresponds to a more complex airy function with more memory effects. As further demonstration of that this behavior may be generic,

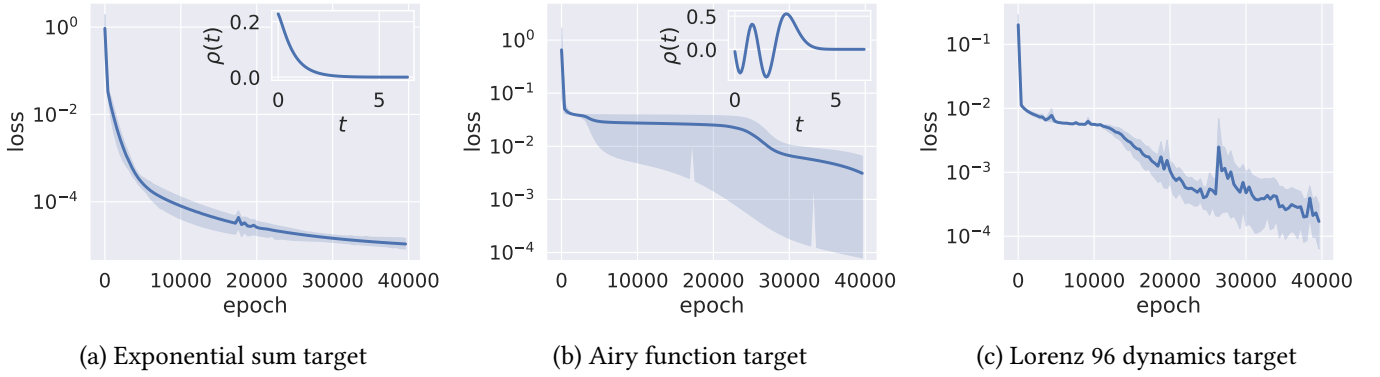


Figure 1: Comparison of gradient descent dynamics on different types of functionals. Here, we set  $m^* = 8$  for the exponential sum example, and  $t_0 = 3, s_0 = 2.25$  for the airy example. In all cases, the trained RNN has hidden dimension 16 and the total length of the path is  $T = 6.4$ . The continuous-time RNNs are discretized using the Euler method with step size 0.1. The last Lorenz example is not a linear functional, and is trained using tanh activations and the Adam optimization method. The shaded region depicts the mean  $\pm$  the standard deviation in 10 independent runs using randomized initialization.

we also consider a nonlinear forced dynamical system, the Lorenz 96 system [Lor96]:

$$\begin{aligned} \dot{y} &= -y + x + \sum_j z_k / K, \\ \dot{z}_k &= 2[z_{k+1}(z_{k-1} - z_{k+2}) - z_k + y], \quad k = 1, \dots, K, \end{aligned} \tag{75}$$

with cyclic indices,  $z_{k+K} = z_k$ .  $x$  is an external stochastic noise. When the unresolved variables  $z_k$  are unknown, the dynamics of the resolved variable  $y$  driven by  $x$  is a nonlinear dynamical system with memory effects. We use a standard nonlinear RNN to learning the sequence-to-sequence mapping  $\mathbf{x}_{0:T} \mapsto \mathbf{y}_{0:T}$ . Figure 1 (c) shows that the training of this system with the presence of memory also exhibits the interesting plateauing phenomenon.

The results in Figure 1 hints at the fact that there are certainly some functionals that are much harder to learn than others, and it is the purpose of the remaining analysis to understand precisely when and why such difficulties occur in simplified but representative settings. In particular, we will again relate this in a precise manner to memory effects in the target functional, which shows yet another facet of the *curse of memory* when it comes to optimization.

**Remark 4.1.** *There are a number of recent results concerning the training of RNNs using gradient methods [HMR18, AZLS19] and they are mostly positive in the sense that trainability is proved under specific settings. Such settings include recovering linear dynamics [HMR18] or over-parameterized settings [AZLS19]. Here, our result concerns the general setting of learning linear functionals that need not come from some underlying linear dynamics, and is also away from the over-parameterized regime. In our case, we discover on the contrary that training can become very difficult even in the linear case, and this can be understood in a quantitative way, as we will now show.*

## 4.2 Dynamical Analysis

It is our goal now to precisely analyze the plateauing behavior and the observed difficulty in training when the target functional possesses certain structures, as shown in Section 4.1. To make analysis amenable, we will make the following simplifications:

- **Simplification 1:** For the inputs, we can take  $\mathbf{x}$  to be the white noise, so that

$$x_{T-t} dt \stackrel{\text{in distribution}}{=} dB_t, \tag{76}$$

where  $B_t$  is the standard  $d$ -dimensional Wiener process. As a consequence, simplifying Equation (73) via Itô's isometry gives

$$J_m(c, W, U) := \mathbb{E}_{\mathbf{x}} J_m(\mathbf{x}; c, W, U) = \int_0^T \left\| c^\top e^{Wt} U - \rho(t)^\top \right\|_2^2 dt, \quad (77)$$

- **Simplification 2:** Note that from previous approximation analysis, it is clear that the spatial dimension plays little role in the overall learning process, since each spatial dimension can be handled separately. Therefore, we focus on the temporal dimension and consider  $d = 1$  in (77). Moreover, we will consider training on large time horizons so we may take  $T \rightarrow \infty$  to get

$$J_m(c, W, b) := \int_0^\infty \left( c^\top e^{Wt} b - \rho(t) \right)^2 dt, \quad (78)$$

where  $\rho(t)$  becomes the scalar-valued ground truth and  $b$  is the sole column of  $U$  before. This corresponds to the so-called single-input-single-output (SISO) system.

- **Simplification 3:** Due to the difficulty of directly analyzing  $\nabla_W e^{Wt}$  and  $\nabla_W^2 e^{Wt}$ , a further simplified ansatz will be considered. We assume that  $W$  is a diagonal matrix with negative entries (such that the system is stable) so that  $W = -\text{diag}(w)$  with  $w > 0$  element-wisely (denoted by  $w \succ 0$ ). Thus, we can combine  $a = b \circ c$  ( $\circ$  denotes the Hadamard product) and rewrite the hypothesis function as

$$\hat{\rho}(t; c, W, b) := c^\top e^{Wt} b = \sum_{i=1}^m a_i e^{-w_i t} =: \hat{\rho}(t; a, w). \quad (79)$$

The optimization problem (78) becomes

$$\min_{a, w \in \mathbb{R}^m, w \succ 0} J_m(a, w) := \int_0^\infty \left( \sum_{i=1}^m a_i e^{-w_i t} - \rho(t) \right)^2 dt, \quad (80)$$

where the target  $\rho \in L^2([0, \infty)) \cap C^2([0, \infty))$  in general. As we will show later, (80) is able to serve as the starting point in the fine-grained theoretical analysis, since it still preserves the plateauing behavior observed in the optimization process. As a further simplification, we will use a continuous-time idealization of the gradient descent dynamics by considering the gradient flow with respect to  $J_m(a, w)$ .

#### 4.2.1 Heuristic Insights from Gradient Flow

We start with some informal discussion on a probable reason behind the plateauing behavior. Let us analyze the gradient flow (indexed by  $\tau$ , a continuous idealization of the GD iterations)

$$\begin{cases} a'(\tau) = -\nabla_a J_m(a(\tau), w(\tau)), \\ w'(\tau) = -\nabla_w J_m(a(\tau), w(\tau)), \end{cases} \quad (81)$$

with some initial conditions  $a(0) = a_0$ ,  $w(0) = w_0 \succ 0$ . A straightforward computation shows that

$$\frac{\partial J_m}{\partial a_k}(a, w) = 2 \int_0^\infty e^{-w_k t} \left( \sum_{i=1}^m a_i e^{-w_i t} - \rho(t) \right) dt, \quad k = 1, 2, \dots, m, \quad (82)$$

$$\frac{\partial J_m}{\partial w_k}(a, w) = 2a_k \int_0^\infty (-t) e^{-w_k t} \left( \sum_{i=1}^m a_i e^{-w_i t} - \rho(t) \right) dt, \quad k = 1, 2, \dots, m. \quad (83)$$

To construct cases when (81) shows plateauing behavior, one can consider in the following situation. When there are plateaus in the training dynamics, the norm  $\|\nabla J_m\|_2$  must be small. To make  $\frac{\partial J_m}{\partial a_k}$  and  $\frac{\partial J_m}{\partial w_k}$  small, a sufficient condition is either  $e^{-w_k t}$ , or the residual  $\hat{\rho}(t; a, w) - \rho(t) = \sum_{i=1}^m a_i e^{-w_i t} - \rho(t)$  is small for each  $t$ .

- If one has a small residual for all  $t$ , a solution is obtained;
- However, if  $e^{-w_k t}$  is small while the residual is large at time  $t$ , one can get small gradients but a high loss

Hence, a plateauing behavior occurs if the residual is large only when  $t$  is large, i.e. the learned functional differs from the target functional at large times. This again relates to long term memory.

Based on this observation, We build this memory effect explicitly into the target functional. Concretely, we consider a ground truth  $\rho$  having the form

$$\rho(t) = \bar{\rho}(t) + \rho_{0,\omega}(t), \quad (84)$$

where  $\bar{\rho}$  is a function which can be approximated well by  $\hat{\rho}(t; a, w)$ , e.g.  $\bar{\rho}$  is the exponential sum  $\sum_{j=1}^{m^*} a_j^* e^{-w_j^* t}$  with  $m^* < m, w_j^* > 0$ ; while  $\rho_{0,\omega}$  is with long-term memory (parameterized by  $\omega$ ), e.g. a spike function with small support on a set with larger and larger  $t$  as  $\omega \rightarrow 0^+$ . In this case, if the initialization is such that  $\hat{\rho} \approx \bar{\rho}$ :

- For small  $t$ , the residual is small;
- For large  $t$ , the residual is not small (but remains bounded), but  $e^{-w_k t}$  will be small.

Both of them give small gradients, but the overall residual (and hence loss) is large. This then leads to the plateauing behavior that we observe in Section 4.1. More importantly, the plateauing time may increase as the memory becomes longer, since  $\hat{\rho}$  tends to first fit the easy to approximate part  $\bar{\rho}$ , and then fit the memory part  $\rho_{0,\omega}$ . A simple example of such a target functional is

$$\rho(t) = a^* e^{-w^* t} + c_0 e^{-\frac{(t-1/\omega)^2}{2\sigma^2}}. \quad (85)$$

where  $w^*, c_0, \sigma > 0$ . This corresponds to the case where  $m^* = 1$ . Observe that as  $\omega \rightarrow 0^+$ , the memory of the sequence of functionals corresponding to  $\rho$  increases. We verify that this simple target functional gives rise to the plateauing behavior observed early for the airy function and the Lorenz system (See Figure 2). We will subsequently quantify this behavior theoretically.

**Remark 4.2.** *As with the approximation results, we emphasize that it is not obvious at all if target functionals in the form of Equation (84) can be generated by an autonomous or forced differential equation. Hence, it is interesting to consider the general case of learning/approximating sequences of functionals as is done here, as opposed to previous approaches of recovering some underlying dynamical system using RNNs [HMR18].*

## 4.2.2 Concrete Dynamical Analysis

Let us implement the ideas proposed in Section 4.2.1 in a precise manner and quantify the plateauing dynamics. The procedure of our analysis is as follows:

1. We consider ground truths of the form (84);
2. We prove that  $J_m$  has a large value but small gradients near the well-approximated part of the ground truth (i.e. when  $\hat{\rho} \approx \bar{\rho}$  in (84));
3. We prove that when  $\hat{\rho} \approx \bar{\rho}$ , the Hessian  $\nabla^2 J_m$  is positive semi-definite when  $\omega = 0$ , but for finite and small  $\omega$  the Hessian has  $\mathcal{O}(1)$  positive eigenvalues and  $o(1)$  negative eigenvalues. This is the most important part in our analysis;
4. Based on these results, we perform a local linearization analysis on the gradient flow (81) for  $\hat{\rho} \approx \bar{\rho}$ , from which the timescale of the plateauing behavior can be derived.

### (1) Ground Truth with Memory



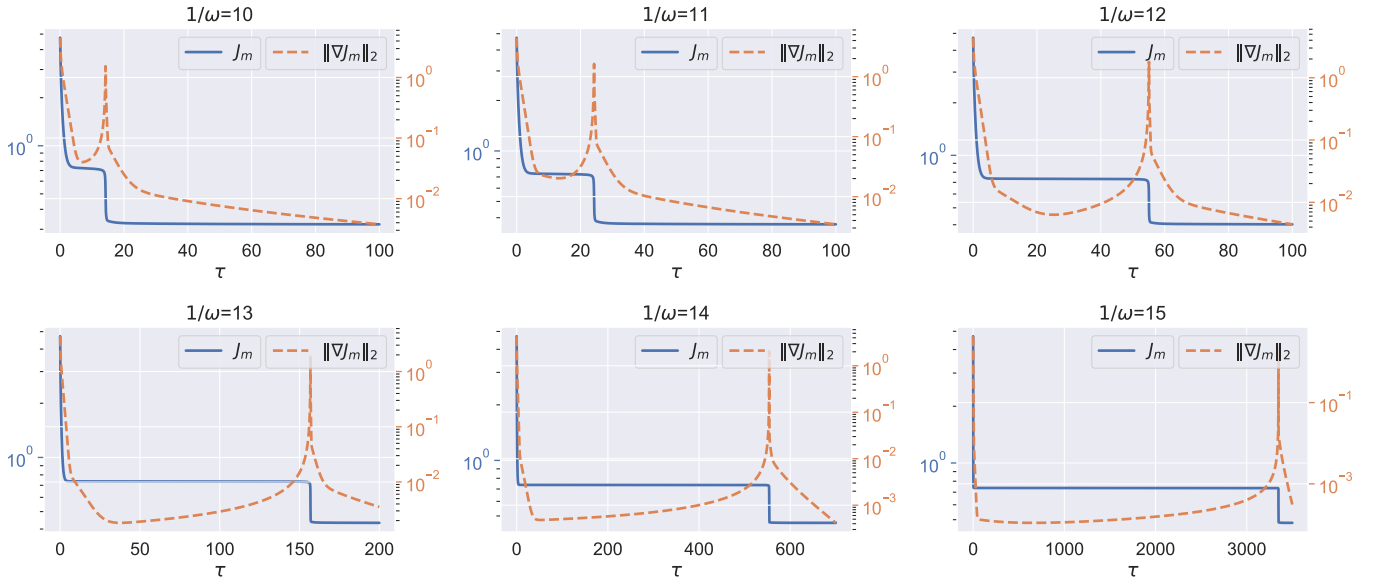


Figure 2: The training dynamics of the target functional defined by Equation (85). Observe that the plateauing time increases rapidly as the memory becomes longer ( $\omega$  decreases). Here, we set  $m = 2$  in the RNN functional  $\hat{\rho}$ . We numerically solve the corresponding gradient flow (81) by the Adams-Bashforth-Moulton method.

We consider the following general form of the ground truth

$$\rho(t) := \bar{\rho}(t) + \rho_{0,\omega}(t) = \sum_{j=1}^{m^*} a_j^* e^{-w_j^* t} + \rho_{0,\omega}(t), \quad (86)$$

where  $a_j^* \neq 0$ ,  $w_j^* > 0$  and  $w_i^* \neq w_j^*$  for any  $i \neq j$ ,  $i, j = 1, \dots, m^*$ , and  $m^* < m$ . The last requirement ensures that the RNN can perfectly represent the first term of the target,  $\bar{\rho}(t)$ . The memory in the system is controlled by the second term, in which we define for  $\omega > 0$ ,

$$\rho_{0,\omega}(t) := \rho_0(t - 1/\omega),$$

with  $\rho_0$  being a fixed template function. As  $\omega \rightarrow 0^+$ , the function's support shifts towards large times, modelling the dominance of long term memory. The following assumptions on  $\rho_0$  are natural.

**Assumptions:** (i)  $\rho_0 \in L^2(\mathbb{R}) \cap C^2(\mathbb{R})$ ; (ii)  $\|\rho_0\|_{L^2[0,\infty)} > 0$ ; (iii)  $\rho_0$  is bounded on  $\mathbb{R}$ , i.e.  $\sup_{t \in \mathbb{R}} |\rho_0(t)| < +\infty$ ; (iv)  $\lim_{t \rightarrow -\infty} \rho_0(t) = 0$ .

**Remark 4.3.** One can easily check a large set of functions satisfies the above assumptions, e.g. the sub-Gaussian function

$$|\rho_0(t)| \leq c_0 e^{-c_1 t^2}, \quad |t| \geq t_0 \quad (87)$$

for some fixed positive constants  $c_0, c_1, t_0$ <sup>1</sup>.

We begin by the following preliminary estimate that is used throughout the subsequent analysis.

**Lemma 4.1.** *Let*

$$\Delta_{n,\omega}(w) := \int_0^\infty t^n e^{-wt} \rho_{0,\omega}(t) dt, \quad w > 0, n \in \mathbb{N}. \quad (88)$$

<sup>1</sup>Obviously, if  $\rho_0$  is proportional to the Gaussian density  $\frac{1}{\sqrt{2\pi}\sigma} e^{-\frac{t^2}{2\sigma^2}}$ , or  $\rho_0$  is any continuous function with compact support on  $[0, \infty)$  (denoted by  $C_c([0, \infty))$ ),  $\rho_0$  is sub-Gaussian. For the corresponding  $\rho_{0,\omega}$ ,  $1/\omega$  denotes respectively the mean of normal distribution and start point of the support interval.

We have  $\lim_{\omega \rightarrow 0^+} \Delta_{n,\omega}(w) = 0$ . In particular, if  $\rho_0$  is sub-Gaussian, we further have

$$\Delta_{n,\omega}(w) = \mathcal{O}\left(\omega^{-n} e^{-w/\omega}\right), \quad \omega \rightarrow 0^+, \quad (89)$$

where  $\mathcal{O}(\cdot)$  hides universal constants only related to  $n, w$ .

*Proof.* Since  $\rho_0$  is bounded on  $\mathbb{R}$ , and  $t^n e^{-wt} \in L^1([0, \infty))$ , by Lebesgue's Dominant Convergence Theorem,

$$\lim_{\omega \rightarrow 0^+} \Delta_{n,\omega}(w) = \int_0^\infty t^n e^{-wt} \cdot \lim_{\omega \rightarrow 0^+} \rho_{0,\omega}(t) dt \stackrel{(iv)}{=} 0, \quad \forall w > 0, \forall n \in \mathbb{N}, \quad (90)$$

where the last equality is due to Assumption (iv). That is, for any  $t \geq 0$ ,

$$\lim_{\omega \rightarrow 0^+} \rho_{0,\omega}(t) = \lim_{\omega \rightarrow 0^+} \rho_0(t - 1/\omega) = \lim_{s \rightarrow -\infty} \rho_0(s) = 0.$$

One can then estimate  $\Delta_{n,\omega}(w)$  under the sub-Gaussian condition (87). Suppose  $0 < \omega < 1/t_0$ , we have

$$\begin{aligned} |\Delta_{n,\omega}(w)| &\leq \int_0^\infty t^n e^{-wt} |\rho_0(t - 1/\omega)| dt \\ &= \int_{1/\omega-t_0}^{1/\omega+t_0} t^n e^{-wt} |\rho_0(t - 1/\omega)| dt + \int_0^{1/\omega-t_0} t^n e^{-wt} |\rho_0(t - 1/\omega)| dt \\ &\quad + \int_{1/\omega+t_0}^\infty t^n e^{-wt} |\rho_0(t - 1/\omega)| dt =: I_1 + I_2 + I_3. \end{aligned}$$

Let  $M_0 := \sup_{t \in \mathbb{R}} |\rho_0(t)| < +\infty$ , then

$$\begin{aligned} I_1 &\leq M_0 \int_{1/\omega-t_0}^{1/\omega+t_0} t^n e^{-wt} dt \leq M_0 e^{-w(1/\omega-t_0)} \int_{1/\omega-t_0}^{1/\omega+t_0} t^n dt \\ &= M_0 e^{wt_0} \cdot e^{-w/\omega} \cdot \frac{(1 + \omega t_0)^{n+1} - (1 - \omega t_0)^{n+1}}{(n+1)\omega^{n+1}} = M_0 e^{wt_0} \omega^{-n} e^{-w/\omega} (2t_0 + \mathcal{O}(\omega)), \quad \omega \rightarrow 0^+, \end{aligned}$$

where  $\mathcal{O}(\cdot)$  hides universal constants only related to  $n$  (with  $t_0$  fixed).

$$I_2 = e^{-w/\omega} \int_{-1/\omega}^{-t_0} (s + 1/\omega)^n e^{-ws} |\rho_0(s)| dt \leq c_0 e^{-w/\omega} \int_{-1/\omega}^{-t_0} (s + 1/\omega)^n e^{-ws} e^{-c_1 s^2} dt,$$

where

$$\begin{aligned} \int_{-1/\omega}^{-t_0} (s + 1/\omega)^n e^{-ws} e^{-c_1 s^2} dt &= e^{\frac{w^2}{4c_1}} \int_{-1/\omega}^{-t_0} (s + 1/\omega)^n e^{-c_1 (s + \frac{w}{2c_1})^2} dt \\ &\leq e^{\sigma^2 w^2 / 2} \int_{\mathbb{R}} (|t| + |1/\omega - \sigma^2 w|)^n \cdot e^{-\frac{t^2}{2\sigma^2}} dt \quad (1/c_1 := 2\sigma^2) \\ &= e^{\sigma^2 w^2 / 2} \sum_{k=0}^n C_n^k (1/\omega - \sigma^2 w)^{n-k} \cdot 2 \int_0^\infty t^k e^{-\frac{t^2}{2\sigma^2}} dt \\ &\leq e^{\sigma^2 w^2 / 2} \sum_{k=0}^n C_n^k (1/\omega)^{n-k} (\sqrt{2}\sigma)^{k+1} \Gamma\left(\frac{k+1}{2}\right) \end{aligned}$$

for any  $0 < \omega < 2c_1/w$ . Here the last inequality utilizes the Mellin Transform of absolute moments of the Gaussian density (see Proposition 1 of [LHC05]). The argument is similar for  $I_3$ , which gives the same bound with  $I_2$ . Therefore, for any  $w > 0, n \in \mathbb{N}$ , taking  $0 < \omega \ll 1$  gives  $|\Delta_{n,\omega}(w)| \leq C_{n,w} \omega^{-n} e^{-w/\omega}$ , where  $C_{n,w} > 0$  is some fixed constant only depending on  $n, w$  (with  $\sigma > 0$  fixed). The proof is completed.  $\square$

## (2) Loss and Gradient

The main idea to show plateauing behavior is to analyze the local dynamics of the gradient flow (81) when  $\hat{\rho} \approx \bar{\rho}$ . To do this, we need to analyze the derivatives of  $J_m$  at  $(a^*, w^*)$  (with degeneracy since  $m > m^*$ ). As we will show later, the loss  $J_m$  remains lower bounded, but  $\|\nabla J_m\|_2$  converges to 0 as  $\omega \rightarrow 0^+$ . This shows that the loss will saturate at a high value.

**Definition 4.1.** For any partition  $\mathcal{P}: \{1, \dots, m\} = \cup_{j=1}^{m^*} \mathcal{I}_j$ , where  $\mathcal{I}_{j_1} \cap \mathcal{I}_{j_2} = \emptyset$  for any  $j_1 \neq j_2, j_1, j_2 = 1, \dots, m^*$ , define the affine space (with respect to  $\mathcal{P}$ )

$$\mathcal{M}_{\mathcal{P}}^* := \left\{ (\hat{a}, \hat{w}) \in \mathbb{R}^m \otimes \mathbb{R}_+^m : \hat{w}_i = w_j^* \text{ for any } i \in \mathcal{I}_j, \sum_{i \in \mathcal{I}_j} \hat{a}_i = a_j^*, \quad j = 1, \dots, m^* \right\}.$$

Define the collection of all such affine spaces  $\mathcal{M}^* := \cup_{\mathcal{P}} \mathcal{M}_{\mathcal{P}}^*$ . Intuitively,  $\mathcal{M}^*$  is the set of equivalent points to  $(a^*, w^*)$  for the purpose of approximation via exponential sums.

**Remark 4.4.** It is straightforward to check that the dimension of each  $\mathcal{M}_{\mathcal{P}}^*$  is  $\sum_{j=1}^{m^*} (|\mathcal{I}_j| - 1) = m - m^*$ . In addition, it can be verified that the cardinality of  $\mathcal{M}^*$  is  $m^*! \binom{m}{m^*}$ , where  $\binom{m}{m^*}$  is the Stirling number of the second kind<sup>2</sup>.

**Proposition 4.1.** For any  $(\hat{a}, \hat{w}) \in \mathcal{M}_{\mathcal{P}}^*$ ,  $J_m(\hat{a}, \hat{w}) \geq \|\rho_0\|_{L^2[0, \infty)}^2 > 0$ . That is, the loss value is lower bounded uniformly in  $\omega$ .

*Proof.* By Definition 4.1 and Assumption (ii), we have

$$\begin{aligned} J_m(\hat{a}, \hat{w}) &= \left\| \sum_{j=1}^{m^*} \sum_{i \in \mathcal{I}_j} \hat{a}_i e^{-\hat{w}_i t} - \sum_{j=1}^{m^*} a_j^* e^{-w_j^* t} - \rho_{0, \omega}(t) \right\|_{L^2[0, \infty)}^2 = \left\| \sum_{j=1}^{m^*} a_j^* e^{-w_j^* t} - \sum_{j=1}^{m^*} a_j^* e^{-w_j^* t} - \rho_{0, \omega}(t) \right\|_{L^2[0, \infty)}^2 \\ &= \|\rho_{0, \omega}\|_{L^2[0, \infty)}^2 \geq \|\rho_0\|_{L^2[0, \infty)}^2 > 0. \end{aligned}$$

□

**Proposition 4.2.** For any bounded subset  $\mathcal{M}_0^* \subset \mathcal{M}_{\mathcal{P}}^*$  and any  $(\hat{a}, \hat{w}) \in \mathcal{M}_0^*$ , we have

$$\|\nabla J_m(\hat{a}, \hat{w})\|_2 = o(1) \quad \text{as} \quad \omega \rightarrow 0^+. \quad (91)$$

In particular, if  $\rho_0$  satisfies the sub-Gaussian condition (87), we further have  $\|\nabla J_m(\hat{a}, \hat{w})\|_2 = \mathcal{O}(\omega^{-1} e^{-c_{w^*}/\omega})$ . Here,  $o(\cdot)$  and  $\mathcal{O}(\cdot)$  hide universal constants related only to  $m, w^*$  and the diameter of  $\mathcal{M}_0^*$ , and  $c_{w^*} > 0$  is a global constant only depending on  $w^*$ .

*Proof.* A straightforward computation shows, for  $k = 1, 2, \dots, m$ ,

$$\frac{\partial J_m}{\partial a_k}(a, w) = 2 \left[ \sum_{i=1}^m \frac{a_i}{w_k + w_i} - \sum_{j=1}^{m^*} \frac{a_j^*}{w_k + w_j^*} \right] - 2\Delta_{0, \omega}(w_k), \quad (92)$$

$$\frac{\partial J_m}{\partial w_k}(a, w) = -2a_k \left[ \sum_{i=1}^m \frac{a_i}{(w_k + w_i)^2} - \sum_{j=1}^{m^*} \frac{a_j^*}{(w_k + w_j^*)^2} \right] + 2a_k \Delta_{1, \omega}(w_k). \quad (93)$$

Notice that for any  $n = 1, 2, \dots$ ,

$$\begin{aligned} \sum_{i=1}^m \frac{\hat{a}_i}{(\hat{w}_k + \hat{w}_i)^n} - \sum_{j=1}^{m^*} \frac{a_j^*}{(\hat{w}_k + w_j^*)^n} &= \sum_{j=1}^{m^*} \sum_{i \in \mathcal{I}_j} \frac{\hat{a}_i}{(\hat{w}_k + \hat{w}_i)^n} - \sum_{j=1}^{m^*} \frac{a_j^*}{(\hat{w}_k + w_j^*)^n} \\ &= \sum_{j=1}^{m^*} \frac{\sum_{i \in \mathcal{I}_j} \hat{a}_i}{(\hat{w}_k + w_j^*)^n} - \sum_{j=1}^{m^*} \frac{a_j^*}{(\hat{w}_k + w_j^*)^n} = 0, \end{aligned} \quad (94)$$

<sup>2</sup>See details in the proof of Theorem A.1.

we get

$$\frac{\partial J_m}{\partial a_k}(\hat{a}, \hat{w}) = -2\Delta_{0,\omega}(\hat{w}_k), \quad \frac{\partial J_m}{\partial w_k}(\hat{a}, \hat{w}) = 2\hat{a}_k\Delta_{1,\omega}(\hat{w}_k).$$

Combining with Lemma 4.1 gives the desired conclusion.  $\square$

### (3) Hessian

The previous analysis justifies the trapping in the plateau. Now, we show that eventually, the dynamics will escape this plateau by showing that, while the Hessian  $\nabla^2 J_m$  becomes positive semi-definite as  $\omega \rightarrow 0^+$  with  $\mathcal{O}(1)$  positive eigenvalues, at sufficiently small but non-zero  $\omega$ , the hessian contains small negative eigenvalues, which results in the eventual escape. Two propositions are given in this regard, which shows respectively the minimal eigenvalue of  $\nabla^2 J_m(\hat{a}, \hat{w})$  is small and negative.

**Proposition 4.3.** *For any bounded subset  $\mathcal{M}_0^* \subset \mathcal{M}_P^*$ , for any  $(\hat{a}, \hat{w}) \in \mathcal{M}_0^*$ , denote the eigenvalues of  $\nabla^2 J_m(\hat{a}, \hat{w})$  by  $\lambda_1 \geq \dots \geq \lambda_{2m}$ , we have*

$$\lambda_1 > 0, \dots, \lambda_{m'} > 0, \lambda_{m'+1} = o(1), \dots, \lambda_{2m} = o(1), \quad \text{as } \omega \rightarrow 0^+,$$

with  $m' \leq 2m^*$ . In particular, if  $\rho_0$  satisfies the sub-Gaussian condition (87), we can further quantify the scale  $o(1)$  by  $\mathcal{O}(\omega^{-2}e^{-c_{w^*}/\omega})$ . Here,  $o(\cdot)$  and  $\mathcal{O}(\cdot)$  hide universal constants only related to  $w^*$  and the diameter of  $\mathcal{M}_0^*$ , and  $c_{w^*} > 0$  is a global constant only depending on  $w^*$ .

*Proof.* A straightforward computation shows, for  $k, l = 1, 2, \dots, m$ ,

$$\frac{\partial^2 J_m}{\partial a_k \partial a_l}(a, w) = \frac{2}{w_k + w_l}, \tag{95}$$

$$\frac{\partial^2 J_m}{\partial a_k \partial w_l}(a, w) = \frac{-2a_l}{(w_k + w_l)^2}, \quad k \neq l, \tag{96}$$

$$\frac{\partial^2 J_m}{\partial a_k \partial w_k}(a, w) = -2 \left[ \sum_{i=1}^m \frac{a_i}{(w_k + w_i)^2} - \sum_{j=1}^{m^*} \frac{a_j^*}{(w_k + w_j^*)^2} \right] - \frac{a_k}{2w_k^2} + 2\Delta_{1,\omega}(w_k), \tag{97}$$

$$\frac{\partial^2 J_m}{\partial w_k \partial w_l}(a, w) = \frac{4a_k a_l}{(w_k + w_l)^3}, \quad k \neq l, \tag{98}$$

$$\frac{\partial^2 J_m}{\partial w_k \partial w_k}(a, w) = 4a_k \left[ \sum_{i=1}^m \frac{a_i}{(w_k + w_i)^3} - \sum_{j=1}^{m^*} \frac{a_j^*}{(w_k + w_j^*)^3} \right] + \frac{a_k^2}{2w_k^3} - 2a_k \Delta_{2,\omega}(w_k). \tag{99}$$

By (94), we have

$$\begin{aligned} \frac{\partial^2 J_m}{\partial a_k \partial a_l}(\hat{a}, \hat{w}) &= \frac{2}{\hat{w}_k + \hat{w}_l}, \\ \frac{\partial^2 J_m}{\partial a_k \partial w_l}(\hat{a}, \hat{w}) &= \frac{-2\hat{a}_l}{(\hat{w}_k + \hat{w}_l)^2} \quad (k \neq l), & \frac{\partial^2 J_m}{\partial a_k \partial w_k}(\hat{a}, \hat{w}) &= -\frac{\hat{a}_k}{2\hat{w}_k^2} + 2\Delta_{1,\omega}(\hat{w}_k), \\ \frac{\partial^2 J_m}{\partial w_k \partial w_l}(\hat{a}, \hat{w}) &= \frac{4\hat{a}_k \hat{a}_l}{(\hat{w}_k + \hat{w}_l)^3} \quad (k \neq l), & \frac{\partial^2 J_m}{\partial w_k \partial w_k}(\hat{a}, \hat{w}) &= \frac{\hat{a}_k^2}{2\hat{w}_k^3} - 2\hat{a}_k \Delta_{2,\omega}(\hat{w}_k). \end{aligned}$$

Let

$$\tilde{J}_m(a, w) := \left\| \sum_{i=1}^m a_i e^{-w_i t} - \sum_{j=1}^{m^*} a_j^* e^{-w_j^* t} \right\|_{L^2[0,\infty)}^2,$$

and

$$\mathcal{E}_\omega(a, w) := \begin{bmatrix} \mathbf{O}_{m \times m} & \text{Diag}(\Delta_{1,\omega}(w)) \\ \text{Diag}(\Delta_{1,\omega}(w)) & -\text{Diag}(\Delta_{2,\omega}(w) \circ a) \end{bmatrix}$$

with  $\Delta_{n,\omega}(w)$  ( $n = 1, 2$ ) performed element-wisely and  $\text{Diag}(x)$  denoting the diagonal matrix with the diagonal vector being  $x$ . Then we have

$$\nabla^2 J_m(a, w) = \nabla^2 \tilde{J}_m(a, w) + 2\mathcal{E}_\omega(a, w). \quad (100)$$

We analyze  $\nabla^2 \tilde{J}_m(\hat{a}, \hat{w})$  and  $\mathcal{E}_\omega(\hat{a}, \hat{w})$  respectively.

a)  $\nabla^2 \tilde{J}_m(\hat{a}, \hat{w})$ :  $\tilde{J}_m(\hat{a}, \hat{w}) = 0$  implies  $\nabla \tilde{J}_m(\hat{a}, \hat{w}) = 0$  and  $\nabla^2 \tilde{J}_m(\hat{a}, \hat{w})$  is positive semi-definite. We further show that  $\nabla^2 \tilde{J}_m(\hat{a}, \hat{w})$  has multiple zero eigenvalues. In fact, since

$$\begin{aligned} \frac{\partial^2 \tilde{J}_m}{\partial a_k \partial a_l}(\hat{a}, \hat{w}) &= \frac{2}{\hat{w}_k + \hat{w}_l}, \\ \frac{\partial^2 \tilde{J}_m}{\partial a_k \partial w_l}(\hat{a}, \hat{w}) &= \frac{-2\hat{a}_l}{(\hat{w}_k + \hat{w}_l)^2} \quad (k \neq l), & \frac{\partial^2 \tilde{J}_m}{\partial a_k \partial w_k}(\hat{a}, \hat{w}) &= -\frac{\hat{a}_k}{2\hat{w}_k^2}, \\ \frac{\partial^2 \tilde{J}_m}{\partial w_k \partial w_l}(\hat{a}, \hat{w}) &= \frac{4\hat{a}_k \hat{a}_l}{(\hat{w}_k + \hat{w}_l)^3} \quad (k \neq l), & \frac{\partial^2 \tilde{J}_m}{\partial w_k \partial w_k}(\hat{a}, \hat{w}) &= \frac{\hat{a}_k^2}{2\hat{w}_k^3}, \end{aligned}$$

it is straightforward to verify that  $\nabla^2 \tilde{J}_m(\hat{a}, \hat{w})^{i,:} = \nabla^2 \tilde{J}_m(\hat{a}, \hat{w})^{j,:}$  and  $\hat{a}_j \cdot \nabla^2 \tilde{J}_m(\hat{a}, \hat{w})^{m+i,:} = \hat{a}_i \cdot \nabla^2 \tilde{J}_m(\hat{a}, \hat{w})^{m+j,:}$  for any  $i, j \in \mathcal{I}_p$ ,  $p = 1, \dots, m^*$ , where  $A^{i,:}$  denotes the  $i$ -th row of matrix  $A$ . That is to say, there are at most  $2m^*$  different rows in  $\nabla^2 \tilde{J}_m(\hat{a}, \hat{w}) \in \mathbb{R}^{2m \times 2m}$ , hence  $\text{rank}(\nabla^2 \tilde{J}_m(\hat{a}, \hat{w})) \leq 2m^*$ . Therefore, the number of zero eigenvalues of  $\nabla^2 \tilde{J}_m(\hat{a}, \hat{w}) \geq \dim \left\{ x \in \mathbb{R}^{2m} : \nabla^2 \tilde{J}_m(\hat{a}, \hat{w}) \cdot x = 0 \right\} = 2m - \text{rank}(\nabla^2 \tilde{J}_m(\hat{a}, \hat{w})) \geq 2(m - m^*)$ . Since  $\nabla^2 \tilde{J}_m(\hat{a}, \hat{w})$  is positive semi-definite, all the nonzero eigenvalues must be positive.

b)  $\mathcal{E}_\omega(\hat{a}, \hat{w})$ : Let  $G_k^{(1)} := \{y \in \mathbb{R} : |y| \leq |\Delta_{1,\omega}(\hat{w}_k)|\}$ , and  $G_k^{(2)} := \{y \in \mathbb{R} : |y + \hat{a}_k \Delta_{2,\omega}(\hat{w}_k)| \leq |\Delta_{1,\omega}(\hat{w}_k)|\}$ . By Gershgorin's Circle Theorem, for any  $\lambda$  being the eigenvalue of  $\mathcal{E}_\omega(\hat{a}, \hat{w})$ ,  $\lambda \in \bigcup_{k=1}^m (G_k^{(1)} \cup G_k^{(2)})$ . This gives  $|\lambda| \leq |\hat{a}_k| |\Delta_{2,\omega}(\hat{w}_k)| + |\Delta_{1,\omega}(\hat{w}_k)|$ ,  $k = 1, \dots, m$ .

Combining with Lemma 4.1 and Weyl's Theorem completes the proof.  $\square$

Now, it remains to show that the smallest eigenvalue is in fact negative, meaning that after a long plateauing time, the system will eventually escape.

**Proposition 4.4.** *Suppose  $m > 2m^*$ ,<sup>3</sup> and  $\Delta_{1,\omega}(w_j^*) \neq 0$  for any  $\omega > 0$ ,  $j = 1, \dots, m^*$ . Then for any  $(\hat{a}, \hat{w}) \in \mathcal{M}_p^*$ ,  $\nabla^2 J_m(\hat{a}, \hat{w})$  has negative eigenvalues.*

*Proof.* By Equation (100),  $\nabla^2 J_m(\hat{a}, \hat{w}) = \nabla^2 \tilde{J}_m(\hat{a}, \hat{w}) + 2\mathcal{E}_\omega(\hat{a}, \hat{w})$ . Denote the eigenvalues of  $\nabla^2 \tilde{J}_m(\hat{a}, \hat{w})$  and  $\mathcal{E}_\omega(\hat{a}, \hat{w})$  by  $\tilde{\lambda}_1 \geq \dots \geq \tilde{\lambda}_{2m}$  and  $\mu_1 \geq \dots \geq \mu_{2m}$  respectively.

a)  $\nabla^2 \tilde{J}_m(\hat{a}, \hat{w})$ : According to the proof of Proposition 4.3,  $\nabla^2 \tilde{J}_m(\hat{a}, \hat{w})$  has at least  $2(m - m^*)$  zero eigenvalues, i.e.  $\tilde{\lambda}_1 > 0, \dots, \tilde{\lambda}_{m'} > 0$  and  $\tilde{\lambda}_{m'+1} = \dots = \tilde{\lambda}_{2m} = 0$  with  $m' \leq 2m^*$ .

b)  $\mathcal{E}_\omega(\hat{a}, \hat{w})$ :  $\Delta_{1,\omega}(w_j^*) \neq 0$  implies that  $\text{Diag}(\Delta_{1,\omega}(\hat{w}))$  is invertible. By the congruent transformation in the form of

$$\begin{bmatrix} I & \mathbf{O} \\ -\frac{1}{2}D_2 D_1^{-1} & I \end{bmatrix} \begin{bmatrix} \mathbf{O} & D_1 \\ D_1 & D_2 \end{bmatrix} \begin{bmatrix} I & -\frac{1}{2}D_1^{-1}D_2 \\ \mathbf{O} & I \end{bmatrix} = \begin{bmatrix} \mathbf{O} & D_1 \\ D_1 & \mathbf{O} \end{bmatrix},$$

<sup>3</sup> $m > 2m^*$  is not necessary for the conclusion to hold. See Remark 4.6

in which  $D_1, D_2$  are diagonal matrices and  $D_1$  is invertible, we know

$$\mathcal{E}_\omega(\hat{a}, \hat{w}) = \begin{bmatrix} \mathbf{O}_{m \times m} & \text{Diag}(\Delta_{1,\omega}(\hat{w})) \\ \text{Diag}(\Delta_{1,\omega}(\hat{w})) & -\text{Diag}(\Delta_{2,\omega}(\hat{w}) \circ \hat{a}) \end{bmatrix},$$

$$\tilde{\mathcal{E}}_\omega(\hat{a}, \hat{w}) := \begin{bmatrix} \mathbf{O}_{m \times m} & \text{Diag}(\Delta_{1,\omega}(\hat{w})) \\ \text{Diag}(\Delta_{1,\omega}(\hat{w})) & \mathbf{O}_{m \times m} \end{bmatrix}$$

have the same index of inertia. One can verify that the eigenvalues of  $\tilde{\mathcal{E}}_\omega(\hat{a}, \hat{w})$  is  $\pm \Delta_{1,\omega}(\hat{w}_i)$  for  $i = 1, \dots, m$ . This gives  $\mu_1 > 0, \dots, \mu_m > 0$  and  $\mu_{m+1} < 0, \dots, \mu_{2m} < 0$ .

By Weyl's Theorem, the minimal eigenvalue of  $\nabla^2 J_m(\hat{a}, \hat{w}) \leq \tilde{\lambda}_j + \mu_k$  for  $j + k \leq 2m + 1$ . Let  $j = m > 2m^* \geq m'$  and  $k = m + 1$ , we have  $\tilde{\lambda}_j = 0$  and  $\mu_k < 0$ , which completes the proof.  $\square$

**Remark 4.5.** Under the assumption of Proposition 4.4 and together with Proposition 4.3, we obtain that  $\nabla^2 J_m(\hat{a}, \hat{w})$  has small and negative eigenvalues for any  $(\hat{a}, \hat{w}) \in \mathcal{M}_0^*$ , where  $\mathcal{M}_0^*$  is any bounded subset of  $\mathcal{M}_P^*$ .

**Remark 4.6.** A simple case below shows that the assumption  $m > 2m^*$  is not necessary. Let  $m = 2, m^* = 1$ . We can directly perform the congruent transformation on  $\nabla^2 J_2(\hat{a}, \hat{w})$ :

$$\nabla^2 J_2(\hat{a}, \hat{w}) = \begin{bmatrix} \frac{1}{w^*} & \frac{1}{w^*} & \frac{-\hat{a}_1}{2w^{*2}} + 2\Delta_{1,\omega}(w^*) & \frac{\hat{a}_1 - a^*}{2w^{*2}} \\ \frac{1}{w^*} & \frac{1}{w^*} & \frac{-\hat{a}_1}{2w^{*2}} & \frac{\hat{a}_1 - a^*}{2w^{*2}} + 2\Delta_{1,\omega}(w^*) \\ \frac{-\hat{a}_1}{2w^{*2}} + 2\Delta_{1,\omega}(w^*) & \frac{-\hat{a}_1}{2w^{*2}} & \frac{\hat{a}_1^2}{2w^{*3}} - 2\hat{a}_1\Delta_{2,\omega}(w^*) & \frac{\hat{a}_1(a^* - \hat{a}_1)}{2w^{*3}} \\ \frac{\hat{a}_1 - a^*}{2w^{*2}} & \frac{\hat{a}_1 - a^*}{2w^{*2}} + 2\Delta_{1,\omega}(w^*) & \frac{\hat{a}_1(a^* - \hat{a}_1)}{2w^{*3}} & \frac{(a^* - \hat{a}_1)^2}{2w^{*3}} - 2(a^* - \hat{a}_1)\Delta_{2,\omega}(w^*) \end{bmatrix}$$

$$\rightarrow \begin{bmatrix} \frac{1}{w^*} & 0 & 0 & 0 \\ 0 & 0 & -2\Delta_{1,\omega}(w^*) & 2\Delta_{1,\omega}(w^*) \\ 0 & -2\Delta_{1,\omega}(w^*) & \frac{\hat{a}_1^2}{4w^{*3}} + 2\left(\frac{\Delta_{1,\omega}(w^*)}{w^*} - \Delta_{2,\omega}(w^*)\right)\hat{a}_1 - 4(\Delta_{2,\omega}(w^*))^2w^* & \frac{\hat{a}_1(a^* - \hat{a}_1)}{4w^{*3}} + \frac{\Delta_{1,\omega}(w^*)}{w^*}(a^* - \hat{a}_1) \\ 0 & 2\Delta_{1,\omega}(w^*) & \frac{\hat{a}_1(a^* - \hat{a}_1)}{4w^{*3}} + \frac{\Delta_{1,\omega}(w^*)}{w^*}(a^* - \hat{a}_1) & \frac{(a^* - \hat{a}_1)^2}{4w^{*3}} - 2(a^* - \hat{a}_1)\Delta_{2,\omega}(w^*) \end{bmatrix}.$$

Since

$$\det \left( \begin{bmatrix} 0 & -2\Delta_{1,\omega}(w^*) & 2\Delta_{1,\omega}(w^*) \\ -2\Delta_{1,\omega}(w^*) & \frac{\hat{a}_1^2}{4w^{*3}} + 2\left(\frac{\Delta_{1,\omega}(w^*)}{w^*} - \Delta_{2,\omega}(w^*)\right)\hat{a}_1 - 4(\Delta_{2,\omega}(w^*))^2w^* & \frac{\hat{a}_1(a^* - \hat{a}_1)}{4w^{*3}} + \frac{\Delta_{1,\omega}(w^*)}{w^*}(a^* - \hat{a}_1) \\ 2\Delta_{1,\omega}(w^*) & \frac{\hat{a}_1(a^* - \hat{a}_1)}{4w^{*3}} + \frac{\Delta_{1,\omega}(w^*)}{w^*}(a^* - \hat{a}_1) & \frac{(a^* - \hat{a}_1)^2}{4w^{*3}} - 2(a^* - \hat{a}_1)\Delta_{2,\omega}(w^*) \end{bmatrix} \right)$$

$$= -4(\Delta_{1,\omega}(w^*))^2 \left( \frac{a^{*2}}{4w^{*3}} + o(1) \right) < 0, \quad \omega \rightarrow 0^+,$$

where  $o(\cdot)$  hides polynomial dependence on  $\Delta_{i,\omega}(w^*)$  for  $i = 1, 2$  (the coefficients are polynomials of  $\hat{a}$ ), we obtain that  $\nabla^2 J_2(\hat{a}, \hat{w})$  has negative eigenvalues for any  $(\hat{a}, \hat{w}) \in \mathcal{M}_0^*$  and  $0 < \omega \ll 1$ .

#### (4) Local Linearization Analysis

The previous analysis can now be tied directly to a quantitative dynamics via linearization arguments. It is shown that under mild assumptions, the gradient flow (81) can become trapped in a plateau with an *exponentially* large timescale, i.e. *the curse of memory* occurs, this time in optimization dynamics instead of approximation rates.

**Theorem 4.1.** Let  $\theta := (a, w)$  and  $\theta(\tau) := (a(\tau), w(\tau))$ . Consider the gradient flow

$$\theta'(\tau) = -\nabla J_m(\theta(\tau)), \quad \theta(0) = (\hat{a}, \hat{w}). \quad (101)$$

Suppose  $\Delta_{n,\omega}(w) = \mathcal{O}(\omega^{-n}e^{-w/\omega})$  as  $\omega \rightarrow 0^+$  for  $n = 0, 1, 2$ ,<sup>4</sup> and the assumptions of Proposition 4.4 holds. Then for any bounded subset  $\mathcal{M}_0^* \subset \mathcal{M}_P^*$  and any  $(\hat{a}, \hat{w}) \in \mathcal{M}_0^*$ , the dynamical system (101) becomes trapped in the plateau with a timescale  $\mathcal{O}(e^{c_{w^*}/\omega} \omega^2 \ln(1/\omega))$  as  $\omega \rightarrow 0^+$ . Here  $\mathcal{O}(\cdot)$  hides universal constants only related to  $m, w^*$  and the diameter of  $\mathcal{M}_0^*$ , and  $c_{w^*} > 0$  is a global constant only depending on  $w^*$ .

<sup>4</sup>The assumption is reasonable according to Lemma 4.1. That is, it can be sufficiently guaranteed by a sub-Gaussian  $\rho_0$ .

*Proof.* Consider the asymptotic expansion with the form

$$\theta(\tau) = \theta_0(\tau) + \sum_{i=1}^{\infty} \delta^i \theta_i(\tau) = \theta_0(\tau) + \delta \theta_1(\tau) + \delta^2 \theta_2(\tau) + o(\delta^2), \quad (102)$$

for some  $\delta \in (0, 1)$  (with  $\delta \ll 1$ ) and  $\theta_i(\tau) = \mathcal{O}(1)$  ( $i = 0, 1, \dots$ ). For consistency, we have  $\theta_0(0) = \theta(0)$  and  $\theta_i(0) = 0$  for  $i = 1, 2, \dots$ . Let  $\tau_0$  be the hitting time

$$\tau_0 := \inf \{ \tau \geq 0 : \|\theta(\tau) - \theta(0)\|_2 > \delta \}. \quad (103)$$

Then by continuity and the definition of infimum,  $\tau_0 > 0$  and  $\|\theta(\tau) - \theta(0)\|_2 \leq \delta$  for any  $\tau \in [0, \tau_0]$ . It is our goal to quantify the scale of  $\tau_0$ .

Let  $g_0 := \nabla J_m(\theta(0))$  and  $H_0 := \nabla^2 J_m(\theta(0))$ . The local linearization on (101) shows

$$\theta'(\tau) = -g_0 - H_0(\theta(\tau) - \theta(0)) + \mathcal{O}(\delta^2), \quad \tau \in [0, \tau_0].$$

Together with (102), we have

$$\begin{aligned} \theta'_0(\tau) &= -g_0 - H_0(\theta_0(\tau) - \theta(0)), & \theta_0(0) &= \theta(0), & \text{at } \mathcal{O}(1) \text{ scale,} \\ \theta'_1(\tau) &= -H_0\theta_1(\tau), & \theta_1(0) &= 0, & \text{at } \mathcal{O}(\delta) \text{ scale,} \\ \theta'_2(\tau) &= -H_0\theta_2(\tau) + \mathcal{O}(1), & \theta_2(0) &= 0, & \text{at } \mathcal{O}(\delta^2) \text{ scale.} \end{aligned}$$

Therefore

$$\begin{aligned} \theta_0(\tau) &= \theta(0) - \left( \int_0^\tau e^{-H_0 s} ds \right) g_0, \\ \theta_1(\tau) &= e^{-H_0 \tau} \theta_1(0) = 0, \end{aligned}$$

which gives

$$\theta(\tau) = \theta(0) - \left( \int_0^\tau e^{-H_0 s} ds \right) g_0 + \mathcal{O}(\delta^2), \quad \tau \in [0, \tau_0]. \quad (104)$$

To achieve a parameter separation gap  $\delta_0$ , i.e.  $\|\theta(\tau) - \theta(0)\|_2 \leq \delta_0$  with  $\delta_0 = \mathcal{O}(\delta)$  and  $\delta_0 \leq \delta$ , we need to take

$$\left\| \left( \int_0^\tau e^{-H_0 s} ds \right) g_0 \right\|_2 = \mathcal{O}(\delta). \quad (105)$$

Let  $H_0 = P^\top \Lambda P$  be the eigenvalue decomposition with  $P$  orthogonal and  $\Lambda = \text{diag}(\lambda_1, \dots, \lambda_{2m})$  consisting of the eigenvalues of  $H_0$  with  $\lambda_1 \geq \dots \geq \lambda_{2m}$ . Then

$$\left\| \left( \int_0^\tau e^{-H_0 s} ds \right) g_0 \right\|_2 = \left\| P^\top \left( \int_0^\tau e^{-\Lambda s} ds \right) P g_0 \right\|_2 \leq \left\| \int_0^\tau e^{-\Lambda s} ds \right\|_2 \|g_0\|_2 = \|g_0\|_2 \max_{1 \leq i \leq 2m} \frac{1}{|\lambda_i|} |e^{-\lambda_i \tau} - 1|.$$

One can easily verify that  $h_\tau(\lambda) := \frac{1}{|\lambda|} |e^{-\lambda \tau} - 1|$ ,  $\tau \geq 0$  monotonically decreases on  $\lambda \in \mathbb{R}$  for any  $\tau \geq 0$ .<sup>5</sup> Hence

$$\left\| \left( \int_0^\tau e^{-H_0 s} ds \right) g_0 \right\|_2 \leq \|g_0\|_2 \frac{1}{|\lambda_{2m}|} |e^{-\lambda_{2m} \tau} - 1|. \quad (106)$$

Let the right hand side of (106) equal to  $\mathcal{O}(\delta)$ , we can obtain a lower bound for the smallest  $\tau$  such that (105) holds. According to Propositions 4.2, 4.3 and 4.4, we have  $\|g_0\|_2 = \mathcal{O}(\omega^{-c_w} e^{-1/\omega})$  and  $0 > \lambda_{2m} = \mathcal{O}(\omega^{-2} e^{-c_w/\omega})$  as

<sup>5</sup>With the convention that  $h_\tau(0) = \tau$  for any  $\tau > 0$  and  $h_0(\lambda) \equiv 0$  for any  $\lambda \in \mathbb{R}$ .

$\omega \rightarrow 0^+$ , where  $\mathcal{O}(\cdot)$  hides universal constants only related to  $m, w^*$  and the diameter of  $\mathcal{M}_0^*$ . For any  $0 < \omega, \delta \ll 1$  with  $\omega = o(\delta)$ , solving RHS of (106) =  $\mathcal{O}(\delta)$  gives

$$\tau \geq \mathcal{O}(e^{c_{w^*}/\omega} \cdot \omega^2 \ln(\delta/\omega)).$$

The last task is to show the dynamics of plateauing of the loss is much slower than the parameter separation. The argument is trivial since for any  $\tau \in [0, \tau_0]$ ,

$$\begin{aligned} J_m(\theta(\tau)) - J_m(\theta(0)) &= g_0^\top (\theta(\tau) - \theta(0)) + (\theta(\tau) - \theta(0))^\top H_0(\theta(\tau) - \theta(0)) + o(\delta^2) \\ &\geq -\|g_0\|_2 \|\theta(\tau) - \theta(0)\|_2 + \lambda_{2m} \|\theta(\tau) - \theta(0)\|_2^2 + o(\delta^2) \\ &= \mathcal{O}\left(\omega^{-1} e^{-c_{w^*}/\omega}\right) \mathcal{O}(\delta) + \mathcal{O}\left(\omega^{-2} e^{-c_{w^*}/\omega}\right) \mathcal{O}(\delta^2) + o(\delta^2) \\ &= o(\delta^2), \quad \omega \rightarrow 0^+. \end{aligned}$$

The proof is completed. □

**Remark 4.7.** *The estimate above is a lower bound on the escape time, so it does not appear to preclude the situation that the plateau will last forever. However, observe that in the proof above, suppose  $\tau_0 = +\infty$  in (103), i.e. the hypothetical situation where the parameters are trapped forever. Write*

$$\tilde{g}_0 = P g_0 = (\tilde{g}_{0,1}, \dots, \tilde{g}_{0,2m}),$$

we have

$$\left\| \left( \int_0^\tau e^{-H_0 s} ds \right) g_0 \right\|_2^2 = \tilde{g}_0^\top \left( \int_0^\tau e^{-\Lambda s} ds \right) \tilde{g}_0 = \sum_{i=1}^{2m} (\tilde{g}_{0,i})^2 (h_\tau(\lambda_i))^2 \geq (\tilde{g}_{0,j})^2 (h_\tau(\lambda_j))^2$$

for any  $j$  such that  $\lambda_j < 0$ . If there is some  $\tilde{g}_{0,j} \neq 0$ , from (104) we get

$$\begin{aligned} \|\theta(\tau) - \theta(0)\|_2 &\geq \left\| \left( \int_0^\tau e^{-H_0 s} ds \right) g_0 \right\|_2 + \mathcal{O}(\delta^2) \\ &\geq \frac{|\tilde{g}_{0,j}|}{-\lambda_j} (e^{-\lambda_j \tau} - 1) + \mathcal{O}(\delta^2) \rightarrow +\infty, \quad \tau \rightarrow +\infty, \end{aligned}$$

which is a contradiction. That is to say, the parameter separation has to achieve a gap  $\delta' > \delta$  within a finite time. This also implies a finite time of plateauing for any  $\omega > 0$ , even if exponentially large.

**Remark 4.8.** *As is shown, the exponential timescale estimate holds regardless of the specific partition  $\mathcal{P}$ . That is to say, the number of qualified affine spaces for initialization  $(\hat{\alpha}, \hat{w}) \in \mathcal{M}_0^* \subset \mathcal{M}_{\mathcal{P}}^*$  is equal to that of partitions, i.e.  $m^*! \binom{m}{m^*}$ , the cardinality of  $\mathcal{M}^*$ . In addition, the initialization sufficiently near these affine spaces is also qualified by continuity.*

**Remark 4.9.** *The dynamical analysis above is generically performed locally. However, motivated by the idea of weights degeneracy (see Definition 4.1), we can further utilize similar methods to give a global landscape analysis on the loss function  $J_m$ . The insight is that this plateauing behavior is likely to occur all over the landscape. See details in Appendix A.*

### 4.2.3 Numerical Verification

#### (1) The Timescale Estimate

First, We numerically verify the timescale proved in Theorem 4.1. That is, the time of plateauing (and also parameter separation  $\|\theta(\tau) - \theta(0)\|_2$ ) is exponentially large as the memory  $1/\omega \rightarrow +\infty$ . The results are shown in Figure 3, where we observe good agreement with the predicted scaling.



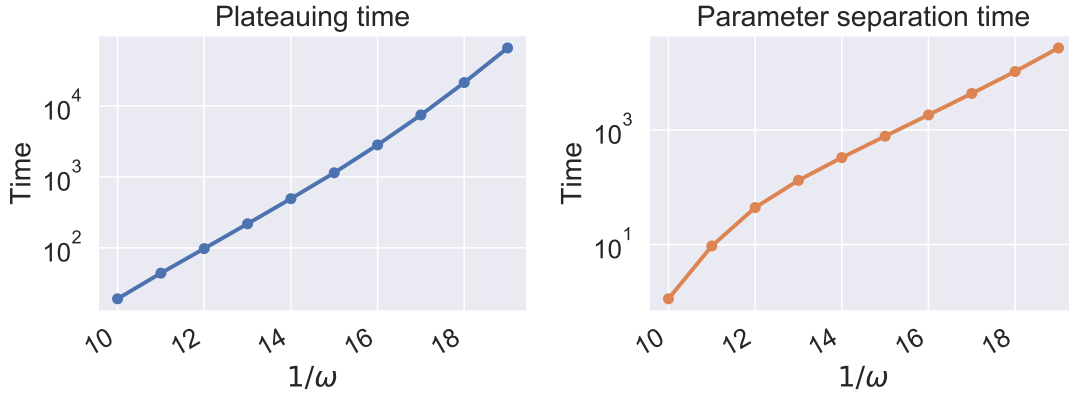


Figure 3: The timescale of plateauing and parameter separation. We see the logarithm of time of plateauing and parameter separation is almost linear to the memory  $1/\omega$ . Here the model and target are both selected the same as Figure 2, but with a larger width  $m = 10$  in order to see corresponding time data under large memories.

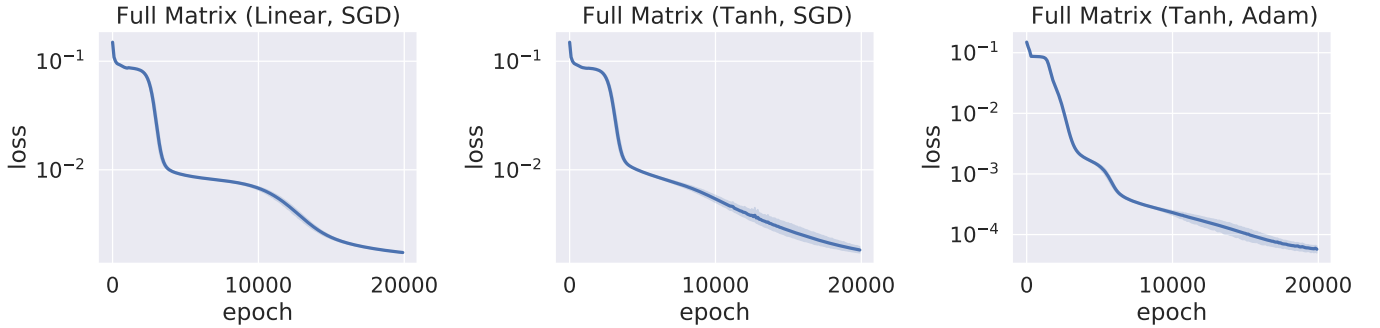


Figure 4: Numerical verification of the plateauing behavior of general cases, with non-diagonal matrices, non-linear activations, and Adam (momentum-based) optimizers. We observe that plateaus happen in all cases and momentum generally improves the situation but does not resolve the difficulty. Here we used the target functional as defined in Figure 2 with  $1/\omega = 20$ . The time horizon is chosen as  $T = 32$ , and 128 input samples are generated from a standard Wiener process. Learning rate for GD is 1.0 and Adam is 0.001. For each experiment, 10 initial conditions are sampled and trained.

## (2) General Case

To facilitate mathematical tractability, the analysis so far is done on the restrictive cases of diagonal  $W$  with negative entries, linear activations and the RNN is optimized with gradient flow. However, we show here that the plateauing behavior - which we now understood as a generic feature of long-term memory of the target functional and its interaction with the optimization landscape - is present even when we consider more general cases, and hence our simplified analytical setting is representative of the general situation. In Figure 4, we take the target functional as described in Equation (85), but apply more general ways to learn it, including using full, non-diagonal matrices in the RNN with no restrictions on entries, using non-linear (tanh) activations and using the Adam optimizer [KB15]. Furthermore, we do not take the Itô isometry simplification and instead use actual input sample paths of finite time horizons, just as one would do in RNNs in practice. We observe that the plateauing behavior is present in all cases. Moreover, in the last case of Adam (which can be thought of as a momentum-based method), the plateauing behavior is somewhat alleviated, although the separation of timescales are still present. This is consistent with our supplemental analysis in Appendix B showing that momentum based methods will speed up training based on our dynamical and landscape analysis of plateauing given here.

#### 4.2.4 The Curse of Memory in Optimization

Let us summarize the findings from the analysis in (1)-(4) of Section 4.2.2. First, the form of the target defined in (1) (see (86)) captures the long term memory in a concrete way. Note that when  $\omega \rightarrow 0^+$ , this corresponds to the case where the influence of target functional  $H_t$  does not decay, much like the case considered in the curse of memory in approximation (Section 3.3). However, different from the approximation case where an exponentially large number of neurons/hidden states is required to achieve approximation, here in optimization the adverse effect of the memory comes with the exponential slow down of gradient flow/descent dynamics. In other words, the plateauing time is now an exponential function of memory, as shown in Theorem 4.1 and verified numerically in Figure 3. We arrived at this by showing that the gradient of the loss function vanishes whereas the Hessian possesses large positive eigenvalues and small, negative eigenvalues, giving rise to the plateauing and escaping behavior. While this is proved under some sensible but restrictive conditions, we show numerically in Section 4.2.3 that this is representative of the general case.

In the literature, a number of results have been obtained pertaining to the analysis of training dynamics of RNN. A positive result for training by GD is established in [HMR18], but this is in the setting of identifying linear systems, i.e. the target functional comes from a linear dynamical system, hence it must possess good decay properties provided it is stable. On the other hand, convergence can also be ensured if the RNN is sufficiently over-parameterized (large  $m$ ) [AZLS19]. However, in reality both of these settings may not be sufficient, and here we provide an alternative analysis of a setting that is representative of the difficulties one may encounter in RNN training. In particular, the curse of memory that we established is consistent with the difficulty in RNN training often observed in practical applications, where heuristic attributions to “memory” is often alluded to [HHAL18, CJGiN<sup>+</sup>17, TV15, LLC<sup>+</sup>18]. The analysis here makes the connection between memory and optimization difficulty precise, and forms a basis for principled development of means to overcome such difficulties in applications.

## 5 Conclusion

In this paper, we analyzed the basic approximation and optimization aspects of using RNN to learn input-output relationships involving temporal sequences in the linear, continuous-time setting. In both cases, our analysis reveals that the dynamical nature of the problem connects the idea of memory and learning in a precise way. In particular, we coined the term *curse of memory*, and revealed two of its facets: When the target relationship to be learned has long term memory, both approximation and optimization become exceedingly difficult. This analysis makes concrete the heuristic observations of the adverse effect of memory on learning with RNNs. Moreover, it quantifies the interaction between the structure of the model (RNN functionals) and the structure of the data (target functionals). The latter is a much less studied topic. More broadly, this approach may be a basic starting point for understanding partially observed time series data in general, including gated RNN variants [HS97, CVMG<sup>+</sup>14] and other methods such as transformers and convolution-based approaches such as WaveNet [VSP<sup>+</sup>17, ODZ<sup>+</sup>16]. These are certainly worthy of future exploration.

## A Landscape Analysis

As mentioned in Remark 4.9, we can perform a global landscape analysis on the loss function based on the idea of weights degeneracy, which arises from Definition 4.1. Recall that the loss function reads

$$\min_{a \in \mathbb{R}^m, w \in \mathbb{R}_+^m} J_m(a, w) := \int_0^\infty \left( \sum_{i=1}^m a_i e^{-w_i t} - \rho(t) \right)^2 dt. \quad (107)$$

The main results of the appendix are summarized as follows.

- In Theorem A.1, we prove that the loss function has infinitely many critical points, which form a factorial number of affine spaces (affine spaces);
- In Theorem A.2, we prove that such (critical) affine spaces are much more than global minimizers provided the target being an exponential sum;<sup>6</sup>
- In Theorem A.3, we prove that on such (critical) affine spaces, the Hessian is singular in the sense of processing multiple zero eigenvalues;
- In Proposition A.1, we prove that the (critical) affine spaces contain both saddles and degenerate stable points which are not global optimal.

Instead of a local dynamical analysis in the main text, we generalize similar methods to a *global landscape analysis* here, and the results hold for the loss function associated with *general targets*. More specifically, these results complement our main results (see Section 4.2.2) in the following aspects.

- It is shown that the weights degeneracy is quite common in the whole landscape of the loss function. Unfortunately, weights degeneracy often worsens the landscape to a large extent;
- It is shown that the weights degeneracy leads to a large number of stable areas (i.e. critical affine spaces), but most of them contribute to non-global minimizers;
- It is shown that these stable areas can also be quite flat, which often connect with local plateaus;
- For the structure of these stable areas, there are both saddles and degenerate critical points (not global optimal). In certain regimes, even saddles can be rather difficult to escape from (see Theorem 4.1).

As a consequence, the optimization problem of linear RNNs is globally and essentially difficult to solve.

## A.1 Symmetry Analysis on the Landscape

This subsection consists of two parts: in subsection A.1.1, we give main results provided the existence of weights degeneracy; in subsection A.1.2, we give sufficient conditions to guarantee the existence. Since the key observation to utilize weights degeneracy is to notice the permutation symmetry of coordinates of gradients, we also called it “symmetry analysis”.

### A.1.1 Generic Theory

We begin with the following definition, which describes the concept of weights degeneracy in a natural and rigorous way.

**Definition A.1.** (*coincided critical solutions and affine spaces*) Let  $d \in \mathbb{N}_+$  and  $1 \leq d \leq m$ . We say  $(a, w)$  is a  $d$ -coincided critical solution of  $J_m$ , if  $\nabla J_m(a, w) = 0$ , and  $w = (w_i) \in \mathbb{R}_+^m$  has  $d$  different components. The coincided critical affine spaces are defined as coincided critical solutions that form affine spaces.

To guarantee the existence of such solutions, it is necessary to have the following definition.

**Definition A.2.**  $(\hat{a}, \hat{w}) \in \mathbb{R}^m \otimes \mathbb{R}_+^m$  is called the non-degenerate global minimizer of  $J_m$ , if and only if

$$J_m(\hat{a}, \hat{w}) = \inf_{a \in \mathbb{R}^m, w \in \mathbb{R}_+^m} J_m(a, w), \quad (108)$$

and  $(\hat{a}, \hat{w})$  takes a non-degenerate form

$$\hat{a}_i \neq 0, \hat{w}_i \neq \hat{w}_j \text{ for } i \neq j, \quad i, j = 1, 2, \dots, m. \quad (109)$$

---

<sup>6</sup>The global minimizers are distinct when the target is an exponential sum. Here we compare the number of (critical) affine spaces with the number of global minimizers (both of them are finite). When the target is not an exponential sum, the same conclusion holds if there are still finite number of global minimizers. See Remark A.3 in subsection A.1.2 for details.

For convenience, we also define an index set

$$\mathcal{N} := \{n \in \mathbb{N}_+ : J_m \text{ has non-degenerate global minimizers for any } m \leq n\}, \quad (110)$$

which is used frequently in the following analysis. For any  $f \in L^2[0, \infty)$ , let  $\mathcal{L}[f]$  be the Laplace transform of  $f$ , i.e.  $\mathcal{L}[f](s) = \int_0^\infty e^{-st} f(t) dt$ ,  $s > 0$ .

We begin with the following lemma.

**Lemma A.1.** *Assume that  $\rho$  is smooth and  $\sqrt{w} |\mathcal{L}[\rho](w)| \rightarrow 0$  as  $w \rightarrow 0^+$  and  $w \rightarrow \infty$ . Then we have  $1 \in \mathcal{N}$  and thus  $\mathcal{N} \neq \emptyset$ .*

*Proof.* We aim to show that there exists  $\hat{a} \neq 0$  and  $\hat{w} > 0$ , such that

$$J_1(\hat{a}, \hat{w}) = \inf_{a \in \mathbb{R}, w \in \mathbb{R}_+} J_1(a, w). \quad (111)$$

The basic idea is to limit the unbounded domain  $a \in \mathbb{R}, w \in \mathbb{R}_+$  to a compact set without effecting the minimization of  $J_1(a, w)$ . We have

$$\begin{aligned} \min_{a, w > 0} J_1(a, w) &= \min_{w > 0} \min_a \left\{ \frac{1}{2w} \cdot a^2 - 2\mathcal{L}[\rho](w) \cdot a + \|\rho\|_{L^2[0, \infty)}^2 \right\} \\ &= \min_{w > 0} \min_a \left\{ \frac{1}{2w} (a - 2w\mathcal{L}[\rho](w))^2 + [\|\rho\|_{L^2[0, \infty)}^2 - 2w(\mathcal{L}[\rho](w))^2] \right\} \\ &= \min_{w > 0} \left\{ \|\rho\|_{L^2[0, \infty)}^2 - 2w(\mathcal{L}[\rho](w))^2 \right\} = J_1(a(w), w), \end{aligned}$$

where  $a(w) := 2w\mathcal{L}[\rho](w)$ . Write  $h(w) := J_1(a(w), w)$ , then  $h(0^+) = h(\infty) = \|\rho\|_{L^2[0, \infty)}^2$ . Obviously  $h(w) < \|\rho\|_{L^2[0, \infty)}^2$  for any  $w > 0$ , hence

$$\min_{w > 0} h(w) = \min_{w \in [w_{lb}, w_{ub}]} h(w), \quad 0 < w_{lb} < w_{ub} < \infty,$$

which implies

$$\min_{a, w > 0} J_1(a, w) = \min_{w > 0} J_1(a(w), w) = \min_{w \in [w_{lb}, w_{ub}]} J_1(a(w), w).$$

That is to say, the minimization of  $J_1(a, w)$  can be equivalently performed on a 2-dimensional smooth curve  $(w, a(w))_{w \in [w_{lb}, w_{ub}]}$ , which is certainly a compact set. By continuity,  $J_1(a, w)$  has global minimizers, say  $(\hat{a}, \hat{w})$ . Obviously  $\hat{w} > 0$  and  $\hat{a} = a(\hat{w}) \neq 0$  (since  $\hat{a} = 0$  implies  $J_1(\hat{a}, w) = \|\rho\|_{L^2[0, \infty)}^2$ , certainly not a minimum), which completes the proof.  $\square$

**Remark A.1.** *If the ground truth is an exponential sum, i.e.  $\rho(t) = \sum_{j=1}^{m^*} a_j^* e^{-w_j^* t}$ , we know  $\rho$  is smooth and  $\sqrt{w} |\mathcal{L}[\rho](w)| \rightarrow 0$  as  $w \rightarrow 0^+$  and  $w \rightarrow \infty$ ; hence  $1 \in \mathcal{N}$  by Lemma A.1, and thus  $\mathcal{N} \neq \emptyset$ . In fact,  $\mathcal{L}[\rho](w) = \sum_{j=1}^{m^*} \frac{a_j^*}{w + w_j^*}$  implies that  $\mathcal{L}[\rho](w) = O(1)$  when  $w \rightarrow 0^+$ , and  $\mathcal{L}[\rho](w) = O(1/w)$  when  $w \rightarrow \infty$ .*

**Theorem A.1.** *Assume that  $\mathcal{N} \neq \emptyset$  with  $\mathcal{N}$  defined as (110). Let  $M := \sup \mathcal{N}$ . Then for any  $m \in \mathbb{N}_+$ ,  $1 \leq d \leq \min\{m, M\}$ , there exists at least  $d! \binom{m}{d}$   $d$ -coincided critical affine spaces of  $J_m$ ,<sup>7</sup> where  $\binom{m}{d} \in \mathbb{N}_+$  is called the Stirling number of the second kind.*

*Proof.* (i) Existence. The key observation is the permutation symmetry of  $\nabla J_m$ : by (82) and (83), if  $a_i = a_j$  and  $w_i = w_j$  for some  $i \neq j$ , then  $\frac{\partial J_m}{\partial a_i} = \frac{\partial J_m}{\partial a_j}$  and  $\frac{\partial J_m}{\partial w_i} = \frac{\partial J_m}{\partial w_j}$ .

<sup>7</sup>Certainly, the affine spaces degenerate to distinct points when  $d = m$ . For sufficient conditions to guarantee  $M > 1$  (to give meaningful results), see Theorem A.6 and Remark A.7 in subsection A.1.2.

For any  $m, d \in \mathbb{N}_+$ ,  $1 \leq d \leq m$ , suppose that  $w = (w_i) \in \mathbb{R}_+^m$  has  $d$  different components. Then for any partition  $\mathcal{P}: \{1, \dots, m\} = \cup_{j=1}^d \mathcal{I}_j$  with  $\mathcal{I}_{j_1} \cap \mathcal{I}_{j_2} = \emptyset$  for any  $j_1 \neq j_2$ ,  $j_1, j_2 = 1, \dots, d$ , define the affine space

$$\mathcal{M}_{\mathcal{P},(b,v),(m,d)} := \left\{ (a, w) \in \mathbb{R}^m \otimes \mathbb{R}_+^m : w_i = v_j \text{ for any } i \in \mathcal{I}_j, \sum_{i \in \mathcal{I}_j} a_i = b_j, \quad j = 1, \dots, d \right\}$$

for some  $(b, v) \in \mathbb{R}^d \otimes \mathbb{R}_+^d$ , where  $v$  has exactly  $d$  different components. Therefore, for any  $(a, w) \in \mathcal{M}_{\mathcal{P},(b,v),(m,d)}$ , we have

$$J_m(a, w) = \left\| \sum_{j=1}^d \sum_{i \in \mathcal{I}_j} a_i e^{-w_i t} - \rho(t) \right\|_{L^2[0, \infty)}^2 = \left\| \sum_{j=1}^d b_j e^{-v_j t} - \rho(t) \right\|_{L^2[0, \infty)}^2 = J_d(b, v),$$

and similarly

$$\begin{aligned} \frac{\partial J_m}{\partial a_k}(a, w) &= 2 \int_0^\infty e^{-v_s t} \left( \sum_{j=1}^d b_j e^{-v_j t} - \rho(t) \right) dt, \quad k \in \mathcal{I}_s, \quad s = 1, 2, \dots, d, \\ \frac{\partial J_m}{\partial w_k}(a, w) &= 2 a_k \int_0^\infty (-t) e^{-v_s t} \left( \sum_{j=1}^d b_j e^{-v_j t} - \rho(t) \right) dt, \quad k \in \mathcal{I}_s, \quad s = 1, 2, \dots, d. \end{aligned}$$

Notice that

$$\begin{aligned} \frac{\partial J_d}{\partial b_s}(b, v) &= 2 \int_0^\infty e^{-v_s t} \left( \sum_{j=1}^d b_j e^{-v_j t} - \rho(t) \right) dt, \quad s = 1, 2, \dots, d, \\ \frac{\partial J_d}{\partial v_s}(b, v) &= 2 b_s \int_0^\infty (-t) e^{-v_s t} \left( \sum_{j=1}^d b_j e^{-v_j t} - \rho(t) \right) dt, \quad s = 1, 2, \dots, d, \end{aligned}$$

we have

$$\frac{\partial J_m}{\partial a_k}(a, w) = \frac{\partial J_d}{\partial b_s}(b, v), \quad b_s \frac{\partial J_m}{\partial w_k}(a, w) = a_k \frac{\partial J_d}{\partial v_s}(b, v), \quad k \in \mathcal{I}_s, \quad s = 1, 2, \dots, d. \quad (112)$$

<sup>8</sup> Since  $d \leq \min\{m, M\}$ ,  $d \in \mathcal{N}$ . In fact, for any  $k \in \mathbb{N}_+$ , if  $k \notin \mathcal{N}$ , there exists  $i \leq k$  such that  $J_{(i)}$  has no non-degenerate global minimizers, we have  $j \notin \mathcal{N}$  for any  $j \geq i$ , hence  $M \leq i - 1 \leq k - 1$ . Hence  $M = \infty$  implies  $\mathcal{N} = \mathbb{N}_+$  and  $M < \infty$  implies  $M \in \mathcal{N}$ , and both of them lead to  $d \in \mathcal{N}$ . Therefore,  $J_d$  has non-degenerate global minimizers, i.e. there exists  $(\hat{b}, \hat{v}) \in \mathbb{R}^d \otimes \mathbb{R}_+^d$  such that

$$J_d(\hat{b}, \hat{v}) = \inf_{b \in \mathbb{R}^d, v \in \mathbb{R}_+^d} J_d(b, v), \quad (113)$$

and  $(\hat{b}, \hat{v})$  takes a non-degenerate form

$$\hat{b}_i \neq 0, \quad \hat{v}_i \neq \hat{v}_j \text{ for any } i \neq j, \quad i, j = 1, 2, \dots, d. \quad (114)$$

By (113), we get  $\nabla J_d(\hat{b}, \hat{v}) = 0$ . Combining with (112) and (114), we obtain  $\nabla J_m(\hat{a}, \hat{w}) = 0$  for any  $(\hat{a}, \hat{w}) \in \mathcal{M}_{\mathcal{P},(\hat{b},\hat{v}),(m,d)}$ , i.e.  $(\hat{a}, \hat{w})$  belongs to a  $d$ -coincided critical affine space. Note that the affine space is with the dimension  $\sum_{j=1}^d (|\mathcal{I}_j| - 1) = m - d$ , since there are  $d$  linear equality constrains on the  $m$ -dimensional vector  $a$ .

<sup>8</sup>By considering the gradient flow dynamic of  $J_d$  instead of  $J_m$ , a model reduction (from  $m$ -dimensional to  $d$ -dimensional) is almost completed on  $\mathcal{M}_{\mathcal{P},(b,v),(m,d)}$ , except for some trivial degenerate cases (e.g.  $a_k = 0$  or  $b_s = 0$ ).

(ii) Counting. By the structure of affine spaces discussed above, we can identify different affine spaces with respect to the partition  $\mathcal{P}$ . For counting the number of different partitions  $\mathcal{P}: \{1, \dots, m\} = \cup_{j=1}^d \mathcal{I}_j$ , it can be decomposed into the following two steps. First, partitioning a set of  $m$  labelled objects into  $d$  nonempty unlabelled subsets. By definition, the answer is the Stirling number of the second kind  $\left\{ \begin{matrix} m \\ d \end{matrix} \right\}$ . Second, assign each partition to  $\mathcal{I}_1, \dots, \mathcal{I}_d$

accordingly. There are  $d!$  ways in total. Therefore, the number of  $d$ -coincided critical affine spaces is at least  $d! \left\{ \begin{matrix} m \\ d \end{matrix} \right\}$ . The proof is completed.  $\square$

Combining Lemma A.1, Remark A.1 and Theorem A.1 gives the following theorem, which states that there are much more saddles and degenerate stable points which are not global optimal than global minimizers in the landscape (provided the target being an exponential sum).

**Theorem A.2.** Fix any  $m \in \mathbb{N}_+$  relatively large. Consider the loss  $J_m$  with the ground truth being a non-degenerate exponential sum, i.e.  $\rho(t) = \sum_{j=1}^m a_j^* e^{-w_j^* t}$ , where  $a_j^* \neq 0$  and  $w_i^* \neq w_j^*$  for any  $i \neq j, i, j = 1, \dots, m$ . Assume that  $m \in \mathcal{N}^9$  with  $\mathcal{N}$  defined in (110). Then in the landscape of  $J_m$ , the number of coincided critical affine spaces is at least  $\text{Poly}(m)$  times larger than the number of global minimizers.

The following simple lemma will be used in the proof of Theorem A.2.

**Lemma A.2.** For any  $m \in \mathbb{N}_+$ ,  $\lambda = (\lambda_1, \dots, \lambda_m)$ ,  $\lambda_i \neq \lambda_j$  for any  $i \neq j, i, j = 1, \dots, m$ , the series of functions  $\{e^{\lambda_i t}\}_{i=1}^m$  is linear independent on any interval  $I \in \mathbb{R}$ .

*Proof.* The aim is to show

$$\sum_{i=1}^m c_i e^{\lambda_i t} = 0, t \in I \Rightarrow c_i = 0, i = 1, \dots, m. \quad (115)$$

(115) holds trivially for  $m = 1$ . Assume that (115) holds for  $m - 1$ , then for any interval  $I \subset \mathbb{R}$ ,

$$\begin{aligned} \sum_{i=1}^m c_i e^{\lambda_i t} = 0, t \in I &\Rightarrow \sum_{i=1}^{m-1} c_i e^{(\lambda_i - \lambda_m)t} + c_m = 0, t \in I \\ &\Rightarrow \sum_{i=1}^{m-1} c_i (\lambda_i - \lambda_m) e^{(\lambda_i - \lambda_m)t} = 0, t \in I. \end{aligned} \quad (116)$$

By induction, we get  $c_i (\lambda_i - \lambda_m) = 0$  for  $i = 1, \dots, m - 1$ . Since  $\lambda_i$ 's are distinct, we have  $c_i = 0$  for  $i = 1, \dots, m - 1$ . Combining with (116), we get  $c_m = 0$ , which completes the proof.  $\square$

*Proof of Theorem A.2.* (i) Global minimizers. Since the ground truth is an exponential sum, we have  $J_m(a, w) \geq 0$  and  $J_m(\bar{a}^*, \bar{w}^*) = 0$ , where  $\bar{a}^* = P a^*$  and  $\bar{w}^* = P w^*$  with  $P \in \mathbb{R}^{m \times m}$  to be some permutation matrix. Next we show  $J_m$  has no other global minimizers.

Suppose  $J_m(a, w) = 0$ , we have

$$\sum_{i=1}^m a_i e^{-w_i t} - \sum_{j=1}^m a_j^* e^{-w_j^* t} = 0, \quad t \geq 0. \quad (117)$$

It is easy to see that for any  $j = 1, \dots, m$ , there exists  $i(j)$  such that  $w_{i(j)} = w_j^*$ . Otherwise, if  $w_i \neq w_j^*, i = 1, \dots, m$ , by (115) or Lemma A.2, we have  $a_j^* = 0$ , which is a contradiction. Notice that  $w_i^* \neq w_j^*$  for any  $i \neq j$ ,

<sup>9</sup>Although the assumption  $m \in \mathcal{N}$  seems strong, we will provide sufficient conditions to guarantee its validity in subsection A.1.2. See an complement in Theorem A.7.

different  $w_j^*$ 's will correspond to different  $w_i$ 's, hence the correspondence is one-to-one. Therefore, let  $w_i = w_{j(i)}^*$ , (117) can be rewritten as

$$0 = \sum_{i=1}^m a_i e^{-w_{j(i)}^* t} - \sum_{i=1}^m a_{j(i)}^* e^{-w_{j(i)}^* t} = \sum_{i=1}^m (a_i - a_{j(i)}^*) e^{-w_{j(i)}^* t}, \quad t \geq 0.$$

Again by Lemma A.2, we have  $a_i = a_{j(i)}^*$ . That is to say,  $J_m(a, w) = 0$  implies  $a = Pa^*$  and  $w = Pw^*$  with  $P \in \mathbb{R}^{m \times m}$  to be some permutation matrix. This gives  $m!$  global minimizers.

(ii) Coincided critical affine spaces. Obviously  $\mathcal{N} \neq \emptyset$ , and  $M = \sup \mathcal{N} \geq m$ . According to Theorem A.1, for any  $d$ ,  $1 \leq d \leq \min\{m, M\} = m$ , we have at least  $d! \binom{m}{d}$   $d$ -coincided critical affine spaces of  $J_m$ . By (i), for any  $d \leq m - 1$ , there are no global minimizers in these affine spaces. Counting the total number

$$\sum_{d=1}^{m-1} d! \binom{m}{d}. \quad (118)$$

(iii) Comparison. To give a bound between (118) and  $m!$ , we need an elementary recurrence

$$\binom{m}{d} = d \binom{m-1}{d} + \binom{m-1}{d-1}.$$

- For  $d = m - 1$ , let  $p_m := \binom{m}{m-1}$ , then

$$p_m = (m-1) \binom{m-1}{m-1} + \binom{m-1}{m-2} = (m-1) + p_{m-1} = \dots = \frac{m(m-1)}{2}.$$

- For  $d = m - 2$ , let  $q_m := \binom{m}{m-2}$ , then

$$\begin{aligned} q_m &= (m-2) \binom{m-1}{m-2} + \binom{m-1}{m-3} = (m-2)p_{m-1} + q_{m-1} = \dots \\ &= \frac{1}{24} [2(m-2)(m-1)(2m-3) + 3(m-2)^2(m-1)^2]. \end{aligned}$$

Combining above gives

$$\frac{1}{m!} \sum_{d=1}^{m-1} d! \binom{m}{d} > \frac{1}{m!} [(m-1)!p_m + (m-2)!q_m] = \frac{(m+1)(3m-2)}{24},$$

which is a quadratic polynomial on  $m$ . The proof is completed.  $\square$

**Remark A.2.** We only take the last two terms of (118) for a lower bound, which is obviously rather loose. In principle, a Poly( $m$ ) bound with higher degrees can be similarly obtained. That is to say, on one hand, there are infinitely many critical points forming affine spaces in the landscape of  $J_m$ ; on the other hand, we see that even only counting the affine spaces, there are still much less global minimizers (given the width  $m$  relatively large).

**Remark A.3.** When the target  $\rho$  is not an exponential sum, it is straightforward to see Theorem A.2 still holds if there are finite number (with the scale of no more than factorial) of global minimizers.

Now we get down to investigate  $\nabla^2 J_m$  on the above coincided critical affine spaces. It is shown that  $\nabla^2 J_m$  is singular and can have multiple zero eigenvalues.

**Theorem A.3.** Fix any  $m, d \in \mathbb{N}_+, 1 \leq d \leq m$ . On the  $d$ -coincided critical affine spaces (induced by non-degenerate global minimizers of  $J_d^{10}$ ) of  $J_m$ ,  $\nabla^2 J_m$  is with rank at most  $m + d$ , and hence has at least  $m - d$  zero eigenvalues.

*Proof.* A straightforward computation shows that, for  $k, l = 1, 2, \dots, m$ ,

$$\frac{\partial^2 J_m}{\partial a_k \partial a_l}(a, w) = \frac{2}{w_k + w_l}, \quad (119)$$

$$\frac{\partial^2 J_m}{\partial a_k \partial w_l}(a, w) = \frac{-2a_l}{(w_k + w_l)^2}, \quad k \neq l, \quad (120)$$

$$\frac{\partial^2 J_m}{\partial a_k \partial w_k}(a, w) = \frac{-a_k}{2w_k^2} + 2 \int_0^\infty (-t)e^{-w_k t} \left( \sum_{i=1}^m a_i e^{-w_i t} - \rho(t) \right) dt. \quad (121)$$

Let the induced  $d$ -coincided critical affine space be  $\mathcal{M}_{\mathcal{P},(\hat{b},\hat{v}),(m,d)}$ , as is derived in the proof of Theorem A.1. Since  $(\hat{b}, \hat{v})$  is the non-degenerate global minimizer of  $J_d$ , we have

$$\begin{aligned} \int_0^\infty (-t)e^{-\hat{w}_k t} \left( \sum_{i=1}^m \hat{a}_i e^{-\hat{w}_i t} - \rho(t) \right) dt &= \int_0^\infty (-t)e^{-\hat{v}_s t} \left( \sum_{j=1}^d \hat{b}_j e^{-\hat{v}_j t} - \rho(t) \right) dt \\ &= \frac{1}{2\hat{b}_s} \frac{\partial J_d}{\partial v_s}(\hat{b}, \hat{v}) = 0, \quad k \in \mathcal{I}_s, \quad s = 1, 2, \dots, d, \end{aligned}$$

for any  $(\hat{a}, \hat{w}) \in \mathcal{M}_{\mathcal{P},(\hat{b},\hat{v}),(m,d)}$ . This gives

$$\frac{\partial^2 J_m}{\partial a_k \partial w_k}(\hat{a}, \hat{w}) = \frac{-\hat{a}_k}{2\hat{w}_k^2}. \quad (122)$$

Now we show that, for any  $i, j \in \mathcal{I}_s, i \neq j, s = 1, 2, \dots, d$ , the  $i$ -th row and  $j$ -th row of  $\nabla^2 J_m(\hat{a}, \hat{w})$  are the same. In fact, for any  $k = 1, \dots, m$ , let  $k \in \mathcal{I}_{s'}$ , then by (119),

$$\frac{\partial^2 J_m}{\partial a_i \partial a_k}(\hat{a}, \hat{w}) = \frac{2}{\hat{w}_i + \hat{w}_k} = \frac{2}{\hat{v}_s + \hat{v}_{s'}}, \quad \frac{\partial^2 J_m}{\partial a_j \partial a_k}(\hat{a}, \hat{w}) = \frac{2}{\hat{w}_j + \hat{w}_k} = \frac{2}{\hat{v}_s + \hat{v}_{s'}}.$$

For  $k \neq i$  and  $k \neq j$ , (120) gives

$$\frac{\partial^2 J_m}{\partial a_i \partial w_k}(\hat{a}, \hat{w}) = \frac{-2\hat{a}_k}{(\hat{w}_i + \hat{w}_k)^2} = \frac{-2\hat{a}_k}{(\hat{v}_s + \hat{v}_{s'})^2}, \quad \frac{\partial^2 J_m}{\partial a_j \partial w_k}(\hat{a}, \hat{w}) = \frac{-2\hat{a}_k}{(\hat{w}_j + \hat{w}_k)^2} = \frac{-2\hat{a}_k}{(\hat{v}_s + \hat{v}_{s'})^2}.$$

Together with (122), for  $k = i \neq j$ ,

$$\frac{\partial^2 J_m}{\partial a_i \partial w_k}(\hat{a}, \hat{w}) = \frac{-\hat{a}_i}{2\hat{w}_i^2} = \frac{-\hat{a}_i}{2\hat{v}_s^2}, \quad \frac{\partial^2 J_m}{\partial a_j \partial w_k}(\hat{a}, \hat{w}) = \frac{-2\hat{a}_i}{(\hat{w}_j + \hat{w}_i)^2} = \frac{-\hat{a}_i}{2\hat{v}_s^2},$$

and similarly for  $k = j \neq i$ ,

$$\frac{\partial^2 J_m}{\partial a_i \partial w_k}(\hat{a}, \hat{w}) = \frac{-2\hat{a}_j}{(\hat{w}_i + \hat{w}_j)^2} = \frac{-\hat{a}_j}{2\hat{v}_s^2}, \quad \frac{\partial^2 J_m}{\partial a_j \partial w_k}(\hat{a}, \hat{w}) = \frac{-\hat{a}_j}{2\hat{w}_j^2} = \frac{-\hat{a}_j}{2\hat{v}_s^2}.$$

That is to say, there are at most  $m + d$  different rows in the symmetric matrix  $\nabla^2 J_m(\hat{a}, \hat{w}) \in \mathbb{R}^{2m \times 2m}$ , hence  $\text{rank}(\nabla^2 J_m(\hat{a}, \hat{w})) \leq m + d$ . Therefore, the number of zero eigenvalues of  $\nabla^2 J_m(\hat{a}, \hat{w}) \geq \dim\{x \in \mathbb{R}^{2m} : \nabla^2 J_m(\hat{a}, \hat{w}) \cdot x = 0\} = 2m - \text{rank}(\nabla^2 J_m(\hat{a}, \hat{w})) \geq m - d$ . The proof is completed.  $\square$

**Remark A.4.** The bound in Theorem A.3 is not sharp. The estimate on  $\text{rank}(\nabla^2 J_m)$  here is loose since only rows with the same elements are considered. In practice (numerical tests), it is often the case that there are more zero eigenvalues of  $\text{rank}(\nabla^2 J_m)$  on the coincided critical affine space  $\mathcal{M}_{\mathcal{P},(\hat{b},\hat{v}),(m,d)}$ .

**Remark A.5.** Theorem A.3 shows that, there are local plateaus around the  $d$ -coincided critical affine spaces  $\mathcal{M}_{\mathcal{P},(\hat{b},\hat{v}),(m,d)}$  for  $d \leq m - 1$ . In addition, the 0-eigenspace of  $J_m$  is higher-dimensional for smaller  $d$ , which may suggest that one can stuck on plateaus more easily.

<sup>10</sup>That is, the affine space  $\mathcal{M}_{\mathcal{P},(\hat{b},\hat{v}),(m,d)}$ . See details in the proof of Theorem A.1



### A.1.2 Sufficient Conditions

There is still a gap when connecting Theorem A.1 and Theorem A.2. That is, it is necessary to guarantee sup  $\mathcal{N}$  relatively large, i.e.  $J_1, J_2, \dots, J_d$  all have non-degenerate global minimizers for  $d$  as large as possible. Motivated by [Kam79], we can give some sufficient conditions by limiting the ground truth  $\rho$  within a smaller function space, the so-called completely monotonic functions.

**Definition A.3.**  $F \in C[0, \infty) \cap C^\infty(0, \infty)$  is called completely monotonic, if and only if

$$(-1)^n F^{(n)}(t) \geq 0, \quad 0 < t < \infty, \quad n = 0, 1, \dots,$$

and  $F(\infty) = 0$ .

**Remark A.6.** Several examples of completely monotonic functions:

- $\rho(t) = 1/(1+t)^\alpha$  for any  $\alpha > 0$ ;
- The non-degenerate exponential sum with positive coefficients

$$\rho(t) = \sum_{j=1}^{m^*} a_j^* e^{-w_j^* t}, \quad 0 \leq w_1^* < \dots < w_{m^*}^*, \quad a_j^* > 0, \quad j = 1, 2, \dots, m^*.$$

Since the space of exponential sums is not close, we turn to consider the problem of finding a best approximation to a given  $\rho \in L^2[0, \infty)$  from the set

$$V_d(\mathbb{R}_+) := \left\{ \hat{\rho} \in C^d[0, \infty) : [(D + w_1) \cdots (D + w_d)] \hat{\rho} = 0 \text{ for some } w_1, \dots, w_d \in \mathbb{R}_+ \right\} \quad (123)$$

with respect to the common  $L^2$ -norm, i.e.  $\inf_{\hat{\rho} \in V_d(\mathbb{R}_+)} \|\hat{\rho} - \rho\|_{L^2[0, \infty)}$ , where  $D$  denotes the common differential operator. Obviously  $V_d(\mathbb{R}_+) \subset L^2[0, \infty)$  and  $V_d(\mathbb{R}_+) \subsetneq V_{d+1}(\mathbb{R}_+)$  for any  $d \in \mathbb{N}_+$ .

[Kam79] proves the following theorem.

**Theorem A.4.** Assume  $\rho \in L^2[0, \infty)$  to be completely monotonic. Then there exists a best approximation  $\hat{\rho}^0$  to  $\rho$  in  $V_d(\mathbb{R}_+)$ , i.e.

$$\|\hat{\rho}^0 - \rho\|_{L^2[0, \infty)} = \inf_{\hat{\rho} \in V_d(\mathbb{R}_+)} \|\hat{\rho} - \rho\|_{L^2[0, \infty)}. \quad (124)$$

When  $\rho \notin V_d(\mathbb{R}_+)$ , any such best approximation admits a non-degenerate form

$$\hat{\rho}^0(t) = \sum_{j=1}^d \hat{b}_j e^{-\hat{v}_j t}, \quad 0 < \hat{v}_1 < \dots < \hat{v}_d, \quad \hat{b}_j > 0, \quad j = 1, 2, \dots, d, \quad (125)$$

and satisfies the generalized Aigrain-Williams equations

$$\mathcal{L}[\hat{\rho}^0](\hat{v}_j) = \mathcal{L}[\rho](\hat{v}_j), \quad j = 1, 2, \dots, d, \quad (126)$$

$$\frac{d}{ds} \mathcal{L}[\hat{\rho}^0](s) \Big|_{s=\hat{v}_j} = \frac{d}{ds} \mathcal{L}[\rho](s) \Big|_{s=\hat{v}_j}, \quad j = 1, 2, \dots, d. \quad (127)$$

Note that (124) and (125) are pretty similar to Definition A.2, except for a different choice of hypothesis function space. Now we show a connection between these two problems.

**Theorem A.5.** Assume  $\rho \in L^2[0, \infty)$  to be completely monotonic, and  $\rho \notin V_d(\mathbb{R}_+)$  for some  $d \in \mathbb{N}_+$ . Then  $J_d$  has non-degenerate global minimizers  $(\hat{b}, \hat{v}) \in \mathbb{R}^d \otimes \mathbb{R}_+^d$ .

*Proof.* According to Theorem A.4, there exists a non-degenerate best approximation  $\hat{\rho}^0$  to  $\rho$  from  $V_d(\mathbb{R}_+)$ , i.e.

$$\|\hat{\rho}^0 - \rho\|_{L^2[0,\infty)} = \inf_{\hat{\rho} \in V_d(\mathbb{R}_+)} \|\hat{\rho} - \rho\|_{L^2[0,\infty)}, \quad (128)$$

$$\hat{\rho}^0(t) = \sum_{j=1}^d \hat{b}_j e^{-\hat{v}_j t}, \quad 0 < \hat{v}_1 < \cdots < \hat{v}_d, \hat{b}_j > 0, j = 1, 2, \dots, d. \quad (129)$$

We aim to prove  $J_d(\hat{b}, \hat{v}) = \inf_{b \in \mathbb{R}^d, v \in \mathbb{R}_+^d} J_d(b, v)$ . Define the following subsets of exponential sums

$$\mathcal{V}_d(\mathbb{R}_+) := \left\{ \hat{\rho} : \hat{\rho}(t) = \sum_{i=1}^d a_i e^{-w_i t}, a_i \in \mathbb{R}, w_i > 0 \right\},$$

$$\mathcal{V}_{d,k}(\mathbb{R}_+) := \left\{ \hat{\rho} \in \mathcal{V}_d(\mathbb{R}_+) : w = (w_i) \text{ has } k \text{ different components} \right\}, \quad 1 \leq k \leq d,$$

then we have  $\inf_{b \in \mathbb{R}^d, v \in \mathbb{R}_+^d} J_d(b, v) = \inf_{\hat{\rho} \in \mathcal{V}_d(\mathbb{R}_+)} \|\hat{\rho} - \rho\|_{L^2[0,\infty)}^2$ . It is straightforward to verify that  $\mathcal{V}_d(\mathbb{R}_+) = \bigcup_{k=1}^d \mathcal{V}_{d,k}(\mathbb{R}_+)$ , and  $\mathcal{V}_{d,k}(\mathbb{R}_+) = \mathcal{V}_{k,k}(\mathbb{R}_+) \subsetneq \mathcal{V}_k(\mathbb{R}_+)$  for  $k = 1, \dots, d$ . By (128), we get

$$\|\hat{\rho}^0 - \rho\|_{L^2[0,\infty)}^2 = \inf_{\hat{\rho} \in V_d(\mathbb{R}_+)} \|\hat{\rho} - \rho\|_{L^2[0,\infty)}^2 \leq \inf_{\hat{\rho} \in \mathcal{V}_{d,d}(\mathbb{R}_+)} \|\hat{\rho} - \rho\|_{L^2[0,\infty)}^2.$$

Since  $\hat{\rho}^0 \in \mathcal{V}_{d,d}(\mathbb{R}_+)$ , we have

$$J_d(\hat{b}, \hat{v}) = \|\hat{\rho}^0 - \rho\|_{L^2[0,\infty)}^2 = \inf_{\hat{\rho} \in \mathcal{V}_{d,d}(\mathbb{R}_+)} \|\hat{\rho} - \rho\|_{L^2[0,\infty)}^2.$$

The last task is to show  $\inf_{\hat{\rho} \in \mathcal{V}_d(\mathbb{R}_+)} \|\hat{\rho} - \rho\|_{L^2[0,\infty)} = \inf_{\hat{\rho} \in \mathcal{V}_{d,d}(\mathbb{R}_+)} \|\hat{\rho} - \rho\|_{L^2[0,\infty)}$ . In fact, for any  $\hat{\rho} \in \mathcal{V}_{k,k}$ ,  $\hat{\rho}(t) = \sum_{i=1}^k a_i e^{-w_i t}$ , let  $\tilde{a} := (a_1, \dots, a_k, 0)$ ,  $\tilde{w} := (w_1, \dots, w_k, 1 + \max_{1 \leq i \leq k} w_i)$ , we get  $\hat{\rho}(t) := \sum_{i=1}^{k+1} \tilde{a}_i e^{-\tilde{w}_i t} \in \mathcal{V}_{k+1,k+1}$ , which implies  $\mathcal{V}_{k,k} \subset \mathcal{V}_{k+1,k+1}$ . Therefore,

$$\begin{aligned} \inf_{\hat{\rho} \in \mathcal{V}_d(\mathbb{R}_+)} \|\hat{\rho} - \rho\|_{L^2[0,\infty)} &= \inf_{\hat{\rho} \in \bigcup_{k=1}^d \mathcal{V}_{d,k}(\mathbb{R}_+)} \|\hat{\rho} - \rho\|_{L^2[0,\infty)} = \min_{1 \leq k \leq d} \left\{ \inf_{\hat{\rho} \in \mathcal{V}_{d,k}(\mathbb{R}_+)} \|\hat{\rho} - \rho\|_{L^2[0,\infty)} \right\} \\ &= \min_{1 \leq k \leq d} \left\{ \inf_{\hat{\rho} \in \mathcal{V}_{k,k}(\mathbb{R}_+)} \|\hat{\rho} - \rho\|_{L^2[0,\infty)} \right\} \geq \inf_{\hat{\rho} \in \mathcal{V}_{d,d}(\mathbb{R}_+)} \|\hat{\rho} - \rho\|_{L^2[0,\infty)}, \end{aligned}$$

which completes the proof.  $\square$

Combining Theorem A.1 and Theorem A.5 immediately gives the following result.

**Theorem A.6.** Assume  $\rho \in L^2[0, \infty)$  to be completely monotonic, and  $\rho \notin V_1(\mathbb{R}_+)$ . Let  $\mathcal{D} := \{d \in \mathbb{N}_+ : \rho \notin V_d(\mathbb{R}_+)\}$ ,  $D_0 := \sup \mathcal{D}$  and write  $m' := \min\{m, D_0\}$ . Then the total number of coincided critical affine spaces of  $J_m$  is at least  $\sum_{d=1}^{m'} d! \begin{Bmatrix} m \\ d \end{Bmatrix}$ .

*Proof.* We have  $1 \in \mathcal{D}$  and thus  $\mathcal{D} \neq \emptyset$ ,  $D_0 \geq 1$ . Since  $V_d(\mathbb{R}_+) \subsetneq V_{d+1}(\mathbb{R}_+)$  for any  $d \in \mathbb{N}_+$ , we have  $\mathcal{D} = \{1, 2, \dots, D_0\}$  if  $D_0 < \infty$ , and  $\mathcal{D} = \mathbb{N}_+$  if  $D_0 = \infty$ .<sup>11</sup> Both of them gives  $\{1, 2, \dots, m'\} \subset \mathcal{D}$ , i.e.  $\rho \notin V_k(\mathbb{R}_+)$  for any  $k \leq m'$ . By Theorem A.5,  $J_{(k)}$  has non-degenerate global minimizers for any  $k \leq m'$ , i.e.  $m' \in \mathcal{N}$ . According to Theorem A.1, for any  $d \in \mathbb{N}_+$ ,  $1 \leq d \leq m' = \min\{m, m'\} \leq \min\{m, M\}$ , there exists at least  $d! \begin{Bmatrix} m \\ d \end{Bmatrix}$   $d$ -coincided

critical affine spaces of  $J_m$ . Sum over  $d$  gives the total number  $\sum_{d=1}^{m'} d! \begin{Bmatrix} m \\ d \end{Bmatrix}$ .  $\square$

<sup>11</sup>In fact,  $V_d(\mathbb{R}_+) \subsetneq V_{d+1}(\mathbb{R}_+)$  for any  $d \in \mathbb{N}_+$  implies if  $\rho \notin V_d(\mathbb{R}_+)$ ,  $\rho \notin V_k(\mathbb{R}_+)$  for any  $k \leq d$ , i.e.  $d \in \mathcal{D} \Rightarrow k \in \mathcal{D}$  for any  $k \leq d$ ; otherwise, if  $\rho \in V_d(\mathbb{R}_+)$ ,  $\rho \in V_l(\mathbb{R}_+)$  for any  $l \geq d$ , i.e.  $d \notin \mathcal{D} \Rightarrow l \notin \mathcal{D}$  for any  $l \geq d$ .

**Remark A.7.** *Examples:*

- Suppose the target is  $\rho(t) = 1/(1+t)^\alpha$ ,  $\alpha > 0$ , then  $\mathcal{D} = \mathbb{N}_+$  and  $D_0 = \infty$ . The total number of coincided critical affine spaces of the corresponding  $J_m$  is at least  $\sum_{d=1}^m d! \binom{m}{d}$ .
- Suppose the target is an non-degenerate exponential sum with positive coefficients:  $\rho(t) = \sum_{j=1}^m a_j^* e^{-w_j^* t}$ , where  $a_j^* > 0$  and  $w_i^* \neq w_j^*$  for any  $i \neq j$ ,  $i, j = 1, \dots, m$ . Then  $\mathcal{D} = \{1, 2, \dots, m-1\}$  and  $D_0 = m-1$ . The total number of coincided critical affine spaces of the corresponding  $J_m$  is at least  $\sum_{d=1}^{m-1} d! \binom{m}{d}$ , which is exactly (118).

An complement for Theorem A.2 is as follows.

**Theorem A.7.** Fix any  $m \in \mathbb{N}_+$  relatively large. Consider the loss  $J_m$  with the ground truth being a non-degenerate exponential sum with positive coefficients, i.e.  $\rho(t) = \sum_{j=1}^m a_j^* e^{-w_j^* t}$ , where  $a_j^* > 0$  and  $w_i^* \neq w_j^*$  for any  $i \neq j$ ,  $i, j = 1, \dots, m$ . Then in the landscape of  $J_m$ , the number of coincided critical affine spaces is at least  $\text{Poly}(m)$  times larger than the number of global minimizers.

*Proof.* By Theorem A.2, the only fact we need to show is  $m \in \mathcal{N}$ . Since  $\rho \in L^2[0, \infty)$  is completely monotonic, and  $\rho \notin V_k(\mathbb{R}_+)$  for any  $k \leq m-1$ , then by Theorem A.5,  $J_{(k)}$  has non-degenerate global minimizers for any  $k \leq m-1$ , i.e.  $m-1 \in \mathcal{N}$ . The proof is completed by noticing that  $J_m$  obviously has non-degenerate global minimizers, e.g.  $(a^*, w^*)$ .  $\square$

### A.1.3 A Low-Dimensional Example

To further understand the structure of coincided critical affine spaces, we focus on a specific low-dimensional example in this subsection. That is

$$\min_{a \in \mathbb{R}^2, w \in \mathbb{R}_+^2} J_2(a, w) = \left\| \sum_{i=1}^2 a_i e^{-w_i t} - \rho(t) \right\|_{L^2[0, \infty)}^2,$$

with the ground truth to be a non-degenerate exponential sum  $\rho(t) = \sum_{j=1}^{m^*} a_j^* e^{-w_j^* t}$ , where  $a_j^* \neq 0$  and  $w_i^* \neq w_j^*$  for any  $i \neq j$ ,  $i, j = 1, \dots, m^*$ . As we will show later, the coincided critical affine spaces of  $J_2$  contain both saddles and degenerate stable points which are not global optimal.

By Lemma A.1, Remark A.1 and Theorem A.1, we know the 1-coincided critical affine space of  $J_2$  exists, and it can be constructed by taking the non-degenerate global minimizer of  $J_1$ , say  $(\hat{a}, \hat{w})$  with  $\hat{a} \neq 0$  and  $\hat{w} > 0$ . Then  $\mathcal{M}_{(\hat{a}, \hat{w}), (2, 1)} := \{(a_1, \hat{a} - a_1, \hat{w}, \hat{w}) : a_1 \in \mathbb{R}\} \in \mathbb{R}^4$  is a line<sup>12</sup>, and  $\nabla J_2(a_1, \hat{a} - a_1, \hat{w}, \hat{w}) = 0$  for any  $a_1 \in \mathbb{R}$ . Denote the Hessian of  $J_2$  on the line  $\mathcal{M}_{(\hat{a}, \hat{w}), (2, 1)}$  by  $\mathcal{A}_{(\hat{a}, \hat{w})}(a_1)$ , i.e.  $\mathcal{A}_{(\hat{a}, \hat{w})}(a_1) := \nabla^2 J_2(a_1, \hat{a} - a_1, \hat{w}, \hat{w})$ . We investigate the landscape of  $J_2$  on the line  $\mathcal{M}_{(\hat{a}, \hat{w}), (2, 1)}$  by analyzing the eigenvalue distribution of  $\mathcal{A}_{(\hat{a}, \hat{w})}(a_1)$ .

**Proposition A.1.** Suppose  $m = m^* = 2$ , and  $0 < w_1^* < w_2^*$ . Let  $I_1 := [0, \hat{a}]$  and  $I_2 := (-\infty, 0) \cup (\hat{a}, +\infty)$ <sup>13</sup>. Then

1. If  $a_1^* a_2^* < 0$ , the minimal eigenvalue of  $\mathcal{A}_{(\hat{a}, \hat{w})}(a_1)$  is 0 for any  $a_1 \in I_1$ , and negative for any  $a_1 \in I_2$ ;
2. If  $a_1^* a_2^* > 0$  and  $w_2^*/w_1^* < 2 + \sqrt{3}$ , the minimal eigenvalue of  $\mathcal{A}_{(\hat{a}, \hat{w})}(a_1)$  is negative for any  $a_1 \in I_1$ , and 0 for any  $a_1 \in I_2$ .

*Proof.* Write  $c(w) := \sum_{j=1}^{m^*} a_j^* \left[ \frac{1}{2w(w+w_j^*)^2} - \frac{1}{(w+w_j^*)^3} \right]$ , and  $a_2 := \hat{a} - a_1$ . A straightforward computation shows

<sup>12</sup>Here we omit the corresponding partition  $\mathcal{P}$  since it is unique.

<sup>13</sup>Suppose  $\hat{a} > 0$  here without loss of generality. If  $\hat{a} < 0$ , we let  $I_1 := [\hat{a}, 0]$  and  $I_2 := (-\infty, \hat{a}) \cup (0, +\infty)$  and the same results hold.

that

$$\mathcal{A}_{(\hat{a}, \hat{w})}(a_1) = \begin{bmatrix} \frac{1}{\hat{w}} & \frac{1}{\hat{w}} & \frac{-a_1}{2\hat{w}^2} & \frac{-a_2}{2\hat{w}^2} \\ \frac{1}{\hat{w}} & \frac{1}{\hat{w}} & \frac{-a_1}{2\hat{w}^2} & \frac{-a_2}{2\hat{w}^2} \\ \frac{-a_1}{2\hat{w}^2} & \frac{-a_1}{2\hat{w}^2} & \frac{a_1^2}{2\hat{w}^3} + 4c(\hat{w})a_1 & \frac{a_1 a_2}{2\hat{w}^3} \\ \frac{-a_2}{2\hat{w}^2} & \frac{-a_2}{2\hat{w}^2} & \frac{a_1 a_2}{2\hat{w}^3} & \frac{a_2^2}{2\hat{w}^3} + 4c(\hat{w})a_2 \end{bmatrix}.$$

Considering the congruent transformation of  $\mathcal{A}_{(\hat{a}, \hat{w})}(a_1)$ , which does not affect the index of inertia:

$$\begin{aligned} \mathcal{A}_{(\hat{a}, \hat{w})}(a_1) &= \begin{bmatrix} \frac{1}{\hat{w}} & \frac{1}{\hat{w}} & \frac{-a_1}{2\hat{w}^2} & \frac{-a_2}{2\hat{w}^2} \\ \frac{1}{\hat{w}} & \frac{1}{\hat{w}} & \frac{-a_1}{2\hat{w}^2} & \frac{-a_2}{2\hat{w}^2} \\ \frac{-a_1}{2\hat{w}^2} & \frac{-a_1}{2\hat{w}^2} & \frac{a_1^2}{2\hat{w}^3} + 4c(\hat{w})a_1 & \frac{a_1 a_2}{2\hat{w}^3} \\ \frac{-a_2}{2\hat{w}^2} & \frac{-a_2}{2\hat{w}^2} & \frac{a_1 a_2}{2\hat{w}^3} & \frac{a_2^2}{2\hat{w}^3} + 4c(\hat{w})a_2 \end{bmatrix} \\ &\rightarrow \begin{bmatrix} \frac{1}{\hat{w}} & 0 & 0 & 0 \\ 0 & 0 & 0 & 0 \\ 0 & 0 & \frac{a_1^2}{4\hat{w}^3} + 4c(\hat{w})a_1 & \frac{a_1 a_2}{4\hat{w}^3} \\ 0 & 0 & \frac{a_1 a_2}{4\hat{w}^3} & \frac{a_2^2}{4\hat{w}^3} + 4c(\hat{w})a_2 \end{bmatrix}, \end{aligned}$$

we see that  $\mathcal{A}_{(\hat{a}, \hat{w})}(a_1)$  has one positive eigenvalue  $1/\hat{w}$  and one eigenvalue 0. What remains are the eigenvalues of

$$\mathcal{A}'_{(\hat{a}, \hat{w})}(a_1) := \begin{bmatrix} \frac{a_1^2}{4\hat{w}^3} + 4c(\hat{w})a_1 & \frac{a_1 a_2}{4\hat{w}^3} \\ \frac{a_1 a_2}{4\hat{w}^3} & \frac{a_2^2}{4\hat{w}^3} + 4c(\hat{w})a_2 \end{bmatrix}. \text{ To determine their signs, we compute}$$

$$\det(\mathcal{A}'_{(\hat{a}, \hat{w})}(a_1)) = a_1(\hat{a} - a_1) \cdot 4c(\hat{w}) \left( \frac{\hat{a}}{4\hat{w}^3} + 4c(\hat{w}) \right) = \frac{1}{\hat{a}^2 \hat{w}^3} a_1(\hat{a} - a_1) \cdot \hat{a}c(\hat{w}) \cdot (\hat{a}^2 + 16\hat{w}^3 \hat{a}c(\hat{w})). \quad (130)$$

So we need to analyze the sign of  $\hat{a}c(\hat{w})$  and  $\hat{a}^2 + 16\hat{w}^3 \hat{a}c(\hat{w})$  under different assumptions on  $(a^*, w^*)$ .

(i)  $a_1^* a_2^* < 0$ . By the optimality condition of  $(\hat{a}, \hat{w})$  for  $J_1$ , we have

$$\hat{a} = 2\hat{w} \sum_{j=1}^{m^*} \frac{a_j^*}{\hat{w} + w_j^*} = 4\hat{w}^2 \sum_{j=1}^{m^*} \frac{a_j^*}{(\hat{w} + w_j^*)^2}, \quad (131)$$

and therefore

$$c(\hat{w}) = \frac{\hat{a}}{8\hat{w}^3} - \sum_{j=1}^{m^*} \frac{a_j^*}{(\hat{w} + w_j^*)^3}.$$

Write  $v_j := w_j^*/\hat{w}$ ,  $j = 1, 2$ , we get  $0 < v_1 < v_2$ , and

$$\hat{a} = 2 \sum_{j=1}^{m^*} \frac{a_j^*}{1 + v_j} = 4 \sum_{j=1}^{m^*} \frac{a_j^*}{(1 + v_j)^2}, \quad \hat{w}^3 c(\hat{w}) = \frac{\hat{a}}{8} - \sum_{j=1}^{m^*} \frac{a_j^*}{(1 + v_j)^3}.$$

Therefore

$$\begin{aligned} 8\hat{w}^3 \hat{a}c(\hat{w}) &= \hat{a}^2 - 8\hat{a} \sum_{j=1}^{m^*} \frac{a_j^*}{(1 + v_j)^3} \\ &= 16 \left[ \sum_{j=1}^{m^*} \frac{a_j^*}{(1 + v_j)^2} \right]^2 - 16 \sum_{j=1}^{m^*} \frac{a_j^*}{1 + v_j} \cdot \sum_{j=1}^{m^*} \frac{a_j^*}{(1 + v_j)^3} \\ &= \frac{-16a_1^* a_2^* (v_1 - v_2)^2}{(1 + v_1)^3 (1 + v_2)^3} \\ &> 0, \end{aligned} \quad (132)$$

which gives  $\hat{a}c(\hat{w}) > 0$  and  $\hat{a}^2 + 16\hat{w}^3\hat{a}c(\hat{w}) > 8\hat{w}^3\hat{a}c(\hat{w}) > 0$ .

(ii)  $a_1^*a_2^* > 0$ ,  $w_2^*/w_1^* < 2 + \sqrt{3}$ . By (132),  $\hat{a}c(\hat{w}) < 0$ .

$$\begin{aligned}
\hat{a}^2 + 16\hat{w}^3\hat{a}c(\hat{w}) &= 3\hat{a}^2 - 16\hat{a} \sum_{j=1}^{m^*} \frac{a_j^*}{(1+v_j)^3} \\
&= 16 \left\{ 3 \left[ \sum_{j=1}^{m^*} \frac{a_j^*}{(1+v_j)^2} \right]^2 - 2 \sum_{j=1}^{m^*} \frac{a_j^*}{1+v_j} \cdot \sum_{j=1}^{m^*} \frac{a_j^*}{(1+v_j)^3} \right\} \\
&= \frac{a_1^{*2}}{u_1^4 u_2^4} [u_2^4 + c^2 u_1^4 + 6cu_1^2 u_2^2 - 2cu_1^3 u_2 - 2cu_1 u_2^3] \quad (c = a_2^*/a_1^*, u_j := 1 + v_j > 1) \\
&= \frac{a_1^{*2}}{u_2^4} (s^4 + c^2 + 6cs^2 - 2cs - 2cs^3) \quad (s = u_2/u_1 > 1) \\
&= \frac{a_1^{*2}}{u_2^4} [c^2 - 2s(s^2 - 3s + 1)c + s^4].
\end{aligned}$$

Since  $4s^2(s^2 - 3s + 1)^2 - 4s^4 = 4s^2(s-1)^2[(s-2)^2 - 3]$ , and  $1 < s = u_2/u_1 = (\hat{w} + w_2^*)/(\hat{w} + w_1^*) < w_2^*/w_1^* < 2 + \sqrt{3}$ , we get  $\Delta_c < 0$ . This implies  $c^2 - 2s(s^2 - 3s + 1)c + s^4 > 0$  and  $\hat{a}^2 + 16\hat{w}^3\hat{a}c(\hat{w}) > 0$ .

In both (i) and (ii),  $\hat{a}^2 + 16\hat{w}^3\hat{a}c(\hat{w}) > 0$ , which implies that there is at least one positive diagonal element of  $\mathcal{A}'_{(\hat{a}, \hat{w})}(a_1)$  in a sufficiently small neighborhood of  $a_1 = 0$  and  $a_1 = \hat{a}$ . By the Rayleigh-Ritz Theorem and Weyl's Theorem,  $\mathcal{A}'_{(\hat{a}, \hat{w})}(a_1)$  has at least one positive eigenvalue in this neighborhood. However, by (130),  $\det(\mathcal{A}'_{(\hat{a}, \hat{w})}(a_1))$  only changes the sign at  $a_1 = 0$  and  $a_1 = \hat{a}$ . This implies another eigenvalue of  $\mathcal{A}'_{(\hat{a}, \hat{w})}(a_1)$  changes the sign at  $a_1 = 0$  and  $a_1 = \hat{a}$  accordingly. By different signs of  $\hat{a}c(\hat{w})$  derived in (i) and (ii), and (130), the proof is completed.  $\square$

**Remark A.8.** From Proposition A.1, we see that there are both saddles and degenerate stable points of  $J_2$  on the critical affine spaces (line)  $\mathcal{M}_{(\hat{a}, \hat{w}), (2,1)}$ , and each of them in fact forms affine spaces (lines) respectively, but they are certainly not global minimizers. Therefore, the gradient-based algorithms can get stuck around this affine space, except that it meets saddles with negative eigenvalues with large magnitude.

## B Momentum Helps Training: Quadratic Examples

In practice, it is often the case that training is trapped in some very flat regions (plateaus), where the loss function has rather small gradients and negative eigenvalues of Hessian. Now we illustrate the escape dynamics (escape from a plateau) via a simple quadratic example.

Consider the loss function  $f(x) = (x_1^2 - \epsilon x_2^2)/2$  with  $0 < \epsilon \ll 1$ . We check the escaping performance for continuous-in-time analogs of two optimization algorithms: gradient decent (GD) and momentum (heavy ball) method.

### (1) Gradient Decent

Consider the gradient flow of  $f(x)$  with an initial value  $x_0 = (\delta, 1)^\top$ , where  $0 < \delta \ll 1$  and  $\delta = O(\epsilon)$ . Thus  $\|\nabla f(x_0)\| = O(\epsilon)$ , and

$$\begin{aligned}
\begin{cases} x_1'(\tau) = -x_1(\tau), & x_1(0) = \delta \\ x_2'(\tau) = \epsilon x_2(\tau), & x_2(0) = 1 \end{cases} &\Rightarrow \begin{cases} x_1(\tau) = \delta e^{-\tau} \\ x_2(\tau) = e^{\epsilon\tau} \end{cases} \\
&\Rightarrow f(x(\tau)) = (\delta^2 e^{-2\tau} - \epsilon e^{2\epsilon\tau})/2 =: \ell_1(\tau).
\end{aligned}$$

It is easy to show that there are different timescales of  $\ell_1(\tau)$ . In fact, when  $\tau = O(1/\epsilon)$ ,  $\ell_1(\tau) = O(\epsilon^2)e^{-|O(1/\epsilon)|} - \epsilon e^{O(1)} = O(\epsilon)$ . However, when  $\tau$  continuous to increase, say

$$\tau \geq \frac{1}{2\epsilon} \ln \frac{\delta_0}{\epsilon} =: \tau_1^\epsilon, \tag{133}$$

where  $\delta_0 > 0$  denotes the gap satisfying  $\epsilon = o(\delta_0)$ , we get  $\ell_1(\tau) \leq \ell_1(\tau_1^\epsilon) = O(\epsilon^2) - \epsilon e^{2\epsilon \cdot \frac{1}{2\epsilon} \ln \frac{\delta_0}{\epsilon}} / 2 = O(\epsilon^2) - \delta_0 / 2 < -\delta_0 / 4$  for any  $\tau \geq \tau_1^\epsilon$ .

## (2) Momentum

The momentum algorithm has the update rule

$$x_{k+1} = x_k - \eta \nabla f(x_k) + \rho(x_k - x_{k-1}), \quad (134)$$

where  $\rho \in \mathbb{R}$ ,  $\eta > 0$  is the learning rate, and  $f$  is the objective. The continuous-in-time analog can be derived as (see e.g. [SBC14] for more details)

$$\begin{aligned} 0 &= \rho \frac{x_{k+1} - 2x_k + x_{k-1}}{\eta} + \frac{(1-\rho)}{\sqrt{\eta}} \frac{x_{k+1} - x_k}{\sqrt{\eta}} + \nabla f(x_k) \\ &\approx \rho x''(t) + \frac{(1-\rho)}{\sqrt{\eta}} x'(t) + \nabla f(x(t)), \end{aligned}$$

with  $x_k := x(k\sqrt{\eta})$  and the step size  $\sqrt{\eta}$  of the simple finite differences<sup>14</sup>. Let  $x_1 = x_0 - \eta \nabla f(x_0)$ , we also get  $x'(0) = -\sqrt{\eta} \nabla f(x(0))$ .

To facilitate a comparison to GD, we take  $\eta = 1$ <sup>15</sup> and  $\rho = 1$ <sup>16</sup>. Plugging the expression of  $f$ , we can solve the ODE

$$\begin{aligned} x''(t) + \nabla f(x(t)) &= 0 \Leftrightarrow \begin{cases} x_1''(\tau) + x_1(\tau) = 0, & x_1(0) = \delta, & x_1'(0) = -\delta \\ x_2''(\tau) - \epsilon x_2(\tau) = 0, & x_2(0) = 1, & x_2'(0) = \epsilon \end{cases} \\ &\Rightarrow \begin{cases} x_1(\tau) = \delta(\cos \tau - \sin \tau) \\ x_2(\tau) = \frac{1+\sqrt{\epsilon}}{2} e^{\sqrt{\epsilon}\tau} + \frac{1-\sqrt{\epsilon}}{2} e^{-\sqrt{\epsilon}\tau} \end{cases} \\ &\Rightarrow f(x(\tau)) = \frac{1}{2} \left[ \delta^2 (\cos \tau - \sin \tau)^2 - \epsilon \left( \frac{1+\sqrt{\epsilon}}{2} e^{\sqrt{\epsilon}\tau} + \frac{1-\sqrt{\epsilon}}{2} e^{-\sqrt{\epsilon}\tau} \right)^2 \right] =: \ell_2(\tau). \end{aligned}$$

It is not hard to show that there are still different timescales of  $\ell_2(\tau)$ . In fact, when  $\tau = O(1/\sqrt{\epsilon})$ ,  $\ell_2(\tau) = O(\epsilon^2)|O(1)| - \epsilon|O(1)|(e^{|O(1)|} + e^{-|O(1)|})^2 = O(\epsilon)$ . However, when  $\tau$  continuous to increase, say

$$\tau \geq \frac{1}{2\sqrt{\epsilon}} \ln \frac{4\delta_0}{\epsilon} =: \tau_2^\epsilon, \quad (135)$$

we get  $\ell_2(\tau_2^\epsilon) = O(\epsilon^2) - \epsilon \left( \frac{1+\sqrt{\epsilon}}{2} \right)^2 e^{2\sqrt{\epsilon}\tau} / 2 + O(\epsilon) = O(\epsilon) - \delta_0 < -\delta_0 / 2$ , hence  $\ell_2(\tau) \leq O(\epsilon) - \delta_0 < -\delta_0 / 2$  for any  $\tau \geq \tau_2^\epsilon$ .

Combining (1) and (2) gives that

- For both dynamics, there are different timescales in the loss function. That is to say, relatively long time is needed to escape the plateaus;
- Compare (133) and (135), we get different timescales for escaping:  $O(1/\epsilon \cdot \ln(1/\epsilon))$  for GD and  $O(1/\sqrt{\epsilon} \cdot \ln(1/\epsilon))$  for momentum. Just like the convex case, where momentum improves the convergence rate by weakening the dependence on condition number, we see momentum can also help to escape rather flat saddles.

<sup>14</sup>It is easy to check the error is of order  $O(\sqrt{\eta})$ .

<sup>15</sup>In the continuous-in-time analog of GD, i.e. gradient flow, the step size is taken as 1.

<sup>16</sup>As is seen later,  $\rho = 1$  not only simplifies the analysis, but also helps to obtain the best acceleration.

## References

- [AZLS19] Zeyuan Allen-Zhu, Yuanzhi Li, and Zhao Song. On the convergence rate of training recurrent neural networks. In *Advances in Neural Information Processing Systems 32*, 2019.
- [BBF<sup>+</sup>99] Pierre Baldi, Søren Brunak, Paolo Frasconi, Giovanni Soda, and Gianluca Pollastri. Exploiting the past and the future in protein secondary structure prediction. *Bioinformatics*, 15(11):937–946, 1999.
- [Bel57] Richard Ernest Bellman. *Dynamic Programming*. Princeton University Press, 1957.
- [Bog07] Vladimir I Bogachev. *Measure theory*, volume 1. Springer Science & Business Media, 2007.
- [Bra86] Dietrich Braess. Approximation by exponential sums. In *Nonlinear Approximation Theory*, pages 168–180. Springer, 1986.
- [BSF94] Yoshua. Bengio, Patrice. Simard, and Paolo. Frasconi. Learning long-term dependencies with gradient descent is difficult. *IEEE Transactions on Neural Networks*, 5(2):157–166, 1994.
- [CAL19] Andrea Ceni, P. Ashwin, and L. Livi. Interpreting recurrent neural networks behaviour via excitable network attractors. *Cognitive Computation*, 12:330–356, 2019.
- [CC93] Tianping Chen and Hong Chen. Approximations of continuous functionals by neural networks with application to dynamical systems. *IEEE Transactions on Neural Networks*, 4:910–918, 1993.
- [CCHC19] Bo Chang, Minmin Chen, Eldad Haber, and Ed H. Chi. AntisymmetricRNN: A dynamical system view on recurrent neural networks. In *International Conference on Learning Representations*, 2019.
- [CJGiN<sup>+</sup>17] Víctor Campos, Brendan Jou, Xavier Giró-i Nieto, Jordi Torres, and Shih-Fu Chang. Skip rnn: Learning to skip state updates in recurrent neural networks. *arXiv preprint arXiv:1708.06834*, 2017.
- [CVMG<sup>+</sup>14] Kyunghyun Cho, Bart Van Merriënboer, Caglar Gulcehre, Dzmitry Bahdanau, Fethi Bougares, Holger Schwenk, and Yoshua Bengio. Learning phrase representations using RNN encoder-decoder for statistical machine translation. *arXiv preprint arXiv:1406.1078*, 2014.
- [CX00] Tommy W. S. Chow and Xiao-Dong Li. Modeling of continuous time dynamical systems with input by recurrent neural networks. *IEEE Transactions on Circuits and Systems I: Fundamental Theory and Applications*, 47(4):575–578, 2000.
- [E17] Weinan E. A Proposal on Machine Learning via Dynamical Systems. *Communications in Mathematics and Statistics*, 5(1):1–11, 2017.
- [GDG<sup>+</sup>15] Karol Gregor, Ivo Danihelka, Alex Graves, Danilo Rezende, and Daan Wierstra. Draw: A recurrent neural network for image generation. volume 37 of *Proceedings of Machine Learning Research*, pages 1462–1471, Lille, France, 07–09 Jul 2015. PMLR.
- [GJ14] Alex Graves and Navdeep Jaitly. Towards end-to-end speech recognition with recurrent neural networks. In *International conference on machine learning*, pages 1764–1772, 2014.
- [GMH13] Alex Graves, Abdel-rahman Mohamed, and Geoffrey Hinton. Speech recognition with deep recurrent neural networks. In *2013 IEEE international conference on acoustics, speech and signal processing*, pages 6645–6649. IEEE, 2013.
- [Gra13] Alex Graves. Generating sequences with recurrent neural networks. *arXiv preprint arXiv:1308.0850*, 2013.
- [GS09] Alex Graves and Jürgen Schmidhuber. Offline handwriting recognition with multidimensional recurrent neural networks. In *Advances in neural information processing systems*, pages 545–552, 2009.

- [Han18] Boris Hanin. Which neural net architectures give rise to exploding and vanishing gradients? In *Advances in Neural Information Processing Systems 31*, pages 582–591. Curran Associates, Inc., 2018.
- [HBFS01] Sepp Hochreiter, Yoshua Bengio, Paolo Frasconi, and Jürgen Schmidhuber. Gradient flow in recurrent nets: the difficulty of learning long-term dependencies. In S. C. Kremer and J. F. Kolen, editors, *A Field Guide to Dynamical Recurrent Neural Networks*. IEEE Press, 2001.
- [HHAL18] Yuhuang Hu, Adrian E. G. Huber, Jithendar Anumula, and Shih-Chii Liu. Overcoming the vanishing gradient problem in plain recurrent networks. *CoRR*, abs/1801.06105, 2018.
- [HKT20] Calypso Herrera, Florian Krach, and Josef Teichmann. Theoretical guarantees for learning conditional expectation using controlled ode-rnn. *ArXiv*, abs/2006.04727, 2020.
- [HMR18] Moritz Hardt, Tengyu Ma, and Benjamin Recht. Gradient descent learns linear dynamical systems. *Journal of Machine Learning Research*, 19(29):1–44, 2018.
- [HR17] Eldad Haber and Lars Ruthotto. Stable architectures for deep neural networks. *Inverse Problems*, 34(1):14004, 2017.
- [HR18] Boris Hanin and David Rolnick. How to start training: The effect of initialization and architecture. In *Advances in Neural Information Processing Systems 31*, pages 571–581. Curran Associates, Inc., 2018.
- [HS97] Sepp Hochreiter and Jürgen Schmidhuber. Long short-term memory. *Neural computation*, 9(8):1735–1780, 1997.
- [iFN93] Ken ichi Funahashi and Yuichi Nakamura. Approximation of dynamical systems by continuous time recurrent neural networks. *Neural Networks*, 6(6):801 – 806, 1993.
- [Jac30] Dunham Jackson. *The theory of approximation*, volume 11. American Mathematical Soc., 1930.
- [Kam76] David W Kammler. Approximation with sums of exponentials in  $L_p[0, \infty)$ . *Journal of Approximation Theory*, 16(4):384–408, April 1976.
- [Kam79] David W. Kammler. Least squares approximation of completely monotonic functions by sums of exponentials. *SIAM Journal on Numerical Analysis*, 16(5):801–818, 1979.
- [KB15] Diederik Kingma and Jimmy Ba. Adam: a method for stochastic optimization. 2015.
- [LCTE17] Qianxiao Li, Long Chen, Cheng Tai, and Weinan E. Maximum principle based algorithms for deep learning. *The Journal of Machine Learning Research*, 18(1):5998–6026, 2017.
- [LH18] Qianxiao Li and Shuji Hao. An Optimal Control Approach to Deep Learning and Applications to Discrete-Weight Neural Networks. In *Proceedings of the 35th International Conference on Machine Learning*, volume 80 of *Proceedings of Machine Learning Research*, pages 2985–2994, Stockholmmsässan, Stockholm Sweden, 2018. PMLR.
- [LHC05] Xiao-Dong Li, John K. L. Ho, and Tommy W. S. Chow. Approximation of dynamical time-variant systems by continuous-time recurrent neural networks. *IEEE Transactions on Circuits and Systems II Analog and Digital Signal Processing*, 52:656–660, 10 2005.
- [Lim20] Soon Hoe Lim. Understanding recurrent neural networks using nonequilibrium response theory. *ArXiv*, abs/2006.11052, 2020.
- [LJK19] Lu Lu, Pengzhan Jin, and G. Karniadakis. Deeponet: Learning nonlinear operators for identifying differential equations based on the universal approximation theorem of operators. *ArXiv*, abs/1910.03193, 2019.
- [LLC<sup>+</sup>18] Shuai Li, Wanqing Li, Chris Cook, Ce Zhu, and Yanbo Gao. Independently recurrent neural network (IndRNN): Building a longer and deeper RNN. *2018 IEEE/CVF Conference on Computer Vision and Pattern Recognition*, pages 5457–5466, 2018.



- [Lor96] Edward N Lorenz. Predictability: A problem partly solved. In *Proc. Seminar on predictability*, volume 1, 1996.
- [Mat93] Michael B. Matthews. Approximating nonlinear fading-memory operators using neural network models. *Circuits, Systems and Signal Processing*, 12:279–307, 1993.
- [Mün14] Ch H Müntz. Über den approximationssatz von weierstrass. In *Mathematische Abhandlungen Hermann Amandus Schwarz*, pages 303–312. Springer, 1914.
- [MWE18] Chao Ma, Jianchun Wang, and Weinan E. Model reduction with memory and the machine learning of dynamical systems. *Communications in Computational Physics*, 25(4):947–962, 2018.
- [NHC19] Murphy Yuezhen Niu, Lior Horesh, and Isaac Chuang. Recurrent neural networks in the eye of differential equations. *ArXiv*, abs/1904.12933, 2019.
- [NN09] Yuichi Nakamura and Masahiro Nakagawa. Approximation capability of continuous time recurrent neural networks for non-autonomous dynamical systems. In *Artificial Neural Networks – ICANN 2009*, pages 593–602, Berlin, Heidelberg, 2009. Springer Berlin Heidelberg.
- [ODZ<sup>+</sup>16] Aaron van den Oord, Sander Dieleman, Heiga Zen, Karen Simonyan, Oriol Vinyals, Alex Graves, Nal Kalchbrenner, Andrew Senior, and Koray Kavukcuoglu. Wavenet: A generative model for raw audio. *arXiv preprint arXiv:1609.03499*, 2016.
- [PMB13] Razvan Pascanu, Tomas Mikolov, and Yoshua Bengio. On the difficulty of training recurrent neural networks. volume 28 of *Proceedings of Machine Learning Research*, pages 1310–1318, Atlanta, Georgia, USA, 17–19 Jun 2013. PMLR.
- [RCD19] Yulia Rubanova, Ricky T. Q. Chen, and David Duvenaud. Latent odes for irregularly-sampled time series. *CoRR*, abs/1907.03907, 2019.
- [RHW86] David E Rumelhart, Geoffrey E Hinton, and Ronald J Williams. Learning representations by back-propagating errors. *nature*, 323(6088):533–536, 1986.
- [SBC14] Weijie Su, Stephen Boyd, and Emmanuel Candes. A differential equation for modeling Nesterov’s accelerated gradient method: Theory and insights. In *Advances in neural information processing systems*, pages 2510–2518, 2014.
- [She18] Alex Sherstinsky. Fundamentals of recurrent neural network (RNN) and long short-term memory (LSTM) network. *ArXiv*, abs/1808.03314, 2018.
- [SP97] Mike Schuster and Kuldeep K Paliwal. Bidirectional recurrent neural networks. *IEEE transactions on Signal Processing*, 45(11):2673–2681, 1997.
- [SZ06] Anton Maximilian Schäfer and Hans Georg Zimmermann. Recurrent neural networks are universal approximators. In Stefanos D. Kollias, Andreas Stafylopatis, W lodzis law Duch, and Erkki Oja, editors, *Artificial Neural Networks – ICANN 2006*, pages 632–640, Berlin, Heidelberg, 2006. Springer Berlin Heidelberg.
- [SZ07] Anton Maximilian Schäfer and Hans-Georg Zimmermann. Recurrent neural networks are universal approximators. *International journal of neural systems*, 17(04):253–263, 2007.
- [Szá16] Otto Szász. Über die approximation stetiger funktionen durch lineare aggregate von potenzen. *Mathematische Annalen*, 77(4):482–496, 1916.
- [TH95] Tianping Chen and Hong Chen. Universal approximation to nonlinear operators by neural networks with arbitrary activation functions and its application to dynamical systems. *IEEE Transactions on Neural Networks*, 6(4):911–917, July 1995.

- [TV15] Sachin S. Talathi and Aniket Vartak. Improving performance of recurrent neural network with relu nonlinearity. *CoRR*, abs/1511.03771, 2015.
- [VSP<sup>+</sup>17] Ashish Vaswani, Noam Shazeer, Niki Parmar, Jakob Uszkoreit, Llion Jones, Aidan N Gomez, Lukasz Kaiser, and Illia Polosukhin. Attention is all you need. In *Advances in neural information processing systems*, pages 5998–6008, 2017.
- [Zwa01] Robert Zwanzig. *Nonequilibrium statistical mechanics*. Oxford University Press, 2001.